The WalRK two-component system is essential for proper cell envelope biogenesis in *Clostridioides difficile*

Ute Müh,[1] Craig D. Ellermeier[1], David S. Weiss[1]

[1]Department of Microbiology and Immunology, University of Iowa, Iowa City, IA 52242

Corresponding authors: craig-ellermeier@uiowa.edu, david-weiss@uiowa.edu

Running title: WalRK is essential in *C. difficile*

Abstract (229 words)

The WalR-WalK two-component regulatory system (TCS) is found in all Firmicutes, where it regulates the expression of multiple genes required for remodeling the cell envelope during growth and division. Unlike most TCSs, WalRK is essential for viability, so it has attracted interest as a potential antibiotic target. Here we used overexpression of WalR and CRISPR interference to investigate the Wal system of *Clostridioides difficile*, a major cause of hospital-associated diarrhea in high-income countries. We confirmed the *wal* operon is essential and identified morphological defects and cell lysis as the major terminal phenotypes of altered *wal* expression. We also used RNA-seq to identify over 150 genes whose expression changes in response to WalR levels. This gene set is enriched in cell envelope genes and includes several predicted PG hydrolases and proteins that could regulate PG hydrolase activity. A distinct feature of the *C. difficile* cell envelope is the presence of an S-layer and we found WalR affects expression of several genes which encode S-layer proteins. An unexpected finding was that some Wal-associated phenotypic defects were inverted in comparison to what has been reported in other Firmicutes. For example, down-regulation of Wal signaling caused *C. difficile* cells to become longer rather than shorter, as in *Bacillus subtilis*. Likewise, down-regulation of Wal rendered *C. difficile* more sensitive to vancomycin, whereas reduced Wal activity is linked to increased vancomycin resistance in *Staphylococcus aureus*.

Importance (100 words)

The WalRK two-component system (TCS) is essential for coordinating synthesis and turnover of peptidoglycan in Firmicutes. Here we investigate the WalRK TCS in *Clostridioides difficile*, an important bacterial pathogen with an atypical cell envelope. We confirmed that WalRK is essential and regulates cell envelope biogenesis, although several of the phenotypic changes we observed were opposite to what has been reported in other Firmicutes. We also identified over 150 genes whose expression is controlled either directly or indirectly by WalR. Overall, our findings provide a foundation for future investigations of an important regulatory system and potential antibiotic target in *C. difficile*.

36 **Introduction**

37 To grow and divide, bacteria must thoroughly remodel their peptidoglycan (PG) sacculus, a large,
38 covalently closed macromolecule that surrounds the cell and provides protection against rupture due to
39 turgor pressure (1). How bacteria remodel the sacculus without making errors that lead to inadvertent
40 lysis is a question that has fascinated microbiologists for decades. The question is also of practical
41 significance because small molecules that undermine normal peptidoglycan biogenesis are among our
42 most effective antibiotics.

43 An important advance in our understanding of cell envelope biogenesis was made over twenty
44 years ago when Fabret and Hoch identified a *Bacillus subtilis* two-component system (TCS) that is
45 essential for viability (2). This TCS is now called the Wal system and is known to coordinate expression
46 of multiple cell envelope genes in the Firmicutes. WalRK is essential in all species studied so far,
47 including pathogens such as *Staphylococcus aureus* (3-5) or *Streptococcus pneumoniae* (6, 7). Because
48 of its essentiality, the Wal TCS has attracted interest as a potential antibiotic target.

49 The Wal TCS comprises the bifunctional kinase/phosphatase WalK together with its cognate
50 response regulator WalR. In addition, *wal* operons typically include genes for membrane proteins known
51 or presumed to modulate WalK activity, but the accessory proteins differ between organisms (8-10).
52 Recent evidence from *B. subtilis* indicates WalK activity is regulated by PG fragments generated by PG
53 hydrolases that open spaces to make room for elongation. These PG fragments bind to WalK's
54 extracellular Cache domain to modulate the phosphorylation state of WalR (11). Phosphorylated WalR
55 in turn binds to various promoters to activate or repress gene expression.

56 The number of genes in the WalR regulon ranges from about a dozen to over 100 (5, 12-16),
57 depending on the species, and only some of these genes are directly activated or repressed by WalR.
58 Although WalR regulons are diverse, they invariably include multiple proteins that contribute to proper
59 biogenesis of the cell envelope, especially PG hydrolases. Consistent with these themes, the phenotypic

60 defects elicited by artificial up- or down-regulation of WalRK signaling include abnormal cell shape, larger
61 cells, smaller cells, ghost cells (lysis), thicker PG, abnormal division septa and altered sensitivity to
62 antibiotics that target PG biogenesis (8-10). In *S. pneumoniae walRK* is essential because it activates
63 expression of an essential PG hydrolase, *pcsB* (6, 7). However, the essentiality of *walRK* in *B. subtilis*
64 and *S. aureus* is polygenic in nature, resulting from abnormal expression of multiple genes that are not
65 by themselves essential. In all three organisms, it is possible to bypass the *walRK* requirement by
66 constitutively expressing one or more Wal regulon PG hydrolases, sometimes in combination with
67 deleting genes for hydrolase inhibitors (6, 17, 18).

68 Here we studied the WalRK TCS to *Clostridioides difficile*, an anaerobic, spore-forming Firmicute
69 responsible for close to a quarter million hospitalizations and over 12,000 deaths per year in the United
70 States (19). Unlike the envelope of most Firmicutes in which *walRK* has been studied previously, the *C.*
71 *difficile* envelope has a proteinaceous S-layer whose assembly presumably must be coordinated with PG
72 synthesis (20-22). In addition, the PG itself is somewhat unusual (23). About 90% of the *N*-
73 acetylglucosamine is deacetylated (which has implications for PG hydrolase activity) and about 70% of
74 the peptide crosslinks are 3-3 rather than 4-3 (which has implications for the structure of PG fragments
75 thought to bind to the Cache domain of WalK (11)). The *C. difficile* Wal system includes a unique
76 lipoprotein gene and a non-canonical WalK that lacks an intracellular PER-ARNT-SIM (PAS) signaling
77 domain (Fig. 1) (10). These features distinguish *C. difficile's* WalRK TCS from those of previously
78 characterized Firmicutes, although a distantly related *wal*-like system in *Mycobacterium tuberculosis*
79 (MtrAB) includes a lipoprotein and a WalK-like histidine kinase without an intracellular PAS domain (10,
80 24, 25). Finally, our recent development of tools for xylose-inducible gene expression and CRISPR
81 interference (26) helped to overcome some of the challenges inherent in phenotypic analysis of essential
82 genes like *walRK* in *C. difficile*.

83

84

85 **Results**

86 **The *wal* operon is required for cell viability, proper rod morphology and intrinsic resistance to**
87 **some antibiotics.** According to Tn-seq, the WalRK TCS is essential in *C. difficile* (27). To confirm and
88 extend this finding, we leveraged the power of CRISPR interference (CRISPRi) for functional analysis of
89 essential genes/operons (28). Our CRISPRi system comprises a xylose-inducible nuclease-defective
90 Cas9, P_{xyl}::*dCas9*, that is targeted to a gene of interest by a single guide RNA expressed constitutively
91 from the glutamate dehydrogenase promoter, P_{gdh}::*sgRNA* (26). Because CRISPRi is polar, we decided
92 to target the first gene in the operon, which encodes a predicted lipoprotein unique to the *C. difficile wal*
93 operon (Fig. 1). We have named this gene *walA.* For reproducibility, we designed two guides against
94 *walA*, sgRNA-*walA1* and sgRNA-*walA2*. Subsequent RNA-seq experiments described below confirmed
95 that targeting dCas9 to *walA* suppressed transcription of the entire operon. As a negative control we used
96 a sgRNA (sgRNA-neg) that does not have a target anywhere on the *C. difficile* chromosome. In some
97 experiments the CRISPRi machinery was produced from a plasmid that confers resistance to
98 thiamphenicol (Thi), while in others it was integrated into the chromosome at the *pyrE* locus in a way that
99 does not leave behind an antibiotic resistance marker (29).

100 Chromosomal- or plasmid-based CRISPRi knockdown of the *wal* operon in either 630Δerm or
101 R20291 reduced viability $\geq 10^4$-fold when cell were plated on TY containing 1% xylose (Fig. 2A and Fig.
102 S1A). Additional phenotypes were characterized in TY broth using 630Δerm derivatives with the CRISPRi
103 machinery integrated at *pyrE*. In the absence of xylose, sgRNA-*waAl1* and sgRNA-*walA2* retarded growth
104 slightly compared to the sgRNA-neg control (Fig. 2B, S1B). This finding indicates there is leaky
105 expression of P_{xyl}::*dCas9,* which was later confirmed by RNA-seq (see below). Under these conditions,
106 cells were on average about 10% longer than wild-type and the fraction of cells with curved or irregular
107 contours increased from ~1% in the sgRNA-neg control to ~20% for sgRNA-*walA1* or ~10% for sgRNA-
108 *walA2* (Fig. 2C-E, S1E,F). Further knockdown of the *wal* operon by addition of xylose exacerbated the
109 growth defect in a dose-dependent manner (Fig. 2B, S1D). In addition, morphological defects became

110 more pronounced, with cells now averaging ~30% longer than controls and up to ~40% exhibiting curved
111 or irregular contours (Fig. 2D,E and S1E,F).

112 Partial knockdown of the *wal* operon in the absence of xylose allowed us to screen for altered
113 sensitivity to antibiotics that target cell envelope biogenesis. We found that the minimal inhibitory
114 concentration (MIC) for ampicillin and daptomycin decreased about 2-fold, while the MIC for vancomycin
115 decreased about 4-fold (Table 1). But sensitivity to the other two cell wall-active antibiotics, imipenem
116 and bacitracin, or the gyrase inhibitor novobiocin was not affected (Table 1).

117

118 **Overexpression of WalR impairs growth, alters morphology and slows autolysis**. We also
119 investigated Wal function in *C. difficile* by overproducing the response regulator WalR to drive cells into
120 an exacerbated Wal-ON state (5, 30). Plating *C. difficile* 630Δerm harboring a P_{xyl}::*walR* expression
121 plasmid onto TY-Thi containing 1% xylose resulted in a 10^6-fold loss of viability (Fig. 3A). This strain failed
122 to grow when subcultured directly into TY-Thi broth containing 1% xylose, but waiting until OD_{600} ~0.2
123 before adding 3% xylose resulted in only a subtle growth defect (Fig. 3B). Three hours post-induction,
124 the cells had become strikingly phase bright and resistant to autolysis when suspended in buffer
125 containing 0.01% Triton X-100 (Fig. 3C,D). Similar results were obtained in the R20291 strain background
126 (Fig. S3).

127 We repeated these experiments after integrating P_{xyl}::*walR* into the chromosome of 630Δerm. As
128 expected, the effects of xylose induction were similar but less pronounced when P_{xyl}::*walR* was in single
129 copy (Fig. 4A). The addition of xylose at subculture was now tolerated and reduced growth in a dose-
130 dependent manner. At 3% xylose, cells became slightly phase-bright. There were some bent or hooked
131 cells, a defect not observed with the P_{xyl}::*walR* plasmid, perhaps because it could only be induced for
132 shorter times. (Fig. 4C). After 6h of induction, cells were harvested and evaluated in the lysis assay. We
133 found that overexpression of *walR* slowed lysis in a dose-dependent manner (Fig. 4B).

134

135 **Expression profiling under Wal-ON conditions.** As a step towards understanding the basis of the
136 various Wal-related phenotypes, we sought to identify the genes in the *wal* regulon. (Note: we use the
137 term regulon for convenience to refer to genes whose expression responds to manipulation of the *wal*
138 operon regardless of whether these effects are direct or indirect.) We began by performing RNA-seq on
139 two strains that overexpress *walR* from a single copy P_{xyl}::*walR* construct integrated at *pyrE*. One of these
140 strains overproduced wild-type WalR, the other overproduced a $WalR^{D66E}$ mutant protein expected to
141 mimic phosphorylated WalR and thus be constitutively active (13, 31). The two strains behaved similarly
142 with respect to growth and performance in the lysis assay (Fig. S4A,B). The control strain for these
143 experiments had the gene for a red fluorescent protein (*rfp*) integrated at *pyrE* (26). Strains were grown
144 overnight in TY, then subcultured into fresh TY at a starting OD_{600} ~0.05. When the OD_{600} reached ~0.2,
145 cultures were induced with 3% xylose and allowed to grow for three hours (~ 2 mass doublings), at which
146 time cells were harvested and processed for RNA-seq. At this time point induction of *walR* had only a
147 small effect on growth rate (Fig. S4A).

148 Not including *walR*, which was induced directly from P_{xyl}, the RNA-seq analysis identified 77
149 genes whose transcript abundance changed ≥4-fold ($p<0.05$) upon overexpression of either *walR* or
150 $walR^{D66E}$ (Table 2). Of these genes, 44 were induced and 33 were repressed. Reassuringly, induction
151 ratios were very similar in the *walR* and $walR^{D66E}$ strains with only two exceptions, *cd630_03901* and
152 *cd630_10631*, both of which encode hypothetical proteins. The 77 genes are predicted by BioCyc (32)
153 to be organized into 65 operons that contain 18 additional genes which missed our 4-fold expression
154 change cut-off. Visual inspection of the expression data revealed these genes almost always trended in
155 the right direction, confirming the predicted structure of most of the operons. We therefore included these
156 18 genes in what we will refer to as the Wal-ON regulon, bringing it to a total of 95 genes in 65 operons
157 (Table 2).

158 Several of the genes and trends in Table 2 are worth highlighting. Xylose induction resulted in a
159 14-fold increase in *walR* mRNA (13-fold for $walR^{D66E}$), while the levels of *walK* or other members of the
160 native operon were not affected. This means that induction of P_{xyl}::*walR* integrated at *pyrE* does not lead

161 to induction of the native *wal* operon, consistent with reports that the *wal* operon is not auto-regulated in
162 other bacteria (8, 16). Another striking feature of Table 2 is the abundance of genes encoding for cell
163 envelope proteins. Of the 95 genes in Table 2, 22 (23%) are predicted to encode exported proteins and
164 29 (31%) are predicted to encode cytoplasmic membrane proteins. For comparison, ~7% of the entire
165 proteome is predicted to be exported and 23% predicted to be membrane proteins (see Methods). Table
166 2 also includes 21 hypotheticals (22% of the total), many of which are likely to be involved in cell envelope
167 processes based on the presence of predicted transmembrane domains or export signals.

168 Peptidoglycan-associated genes, especially PG hydrolases, are prominent members of the Wal
169 regulon in all Firmicutes examined to date (8, 10), and *C. difficile* is no exception. Table 2 lists ten
170 peptidoglycan-associated genes, including the second most highly induced gene, *pgdA*, which was
171 upregulated 16-fold. PgdA deacetylates N-acetylglucosamine in peptidoglycan, and is important for *C.*
172 *difficile's* high lysozyme resistance (33, 34). AsnB (~8-fold induced) is annotated as an asparagine
173 synthetase, but its primary function is to amidate diaminopimelic acid in PG stem peptides (35). In *B.*
174 *subtilis*, amidation of m-DAP inhibits PG hydrolase activity (36). MurE (7-fold repressed) catalyzes one
175 of the cytoplasmic steps in PG synthesis, addition of diaminopimelic acid to the nucleotide-linked PG
176 precursor (37). Down regulation of *murE* suggests PG synthesis may be decreased in Wal-ON conditions.
177 Cwp16 and Cwp17 are S-layer proteins with predicted amidase domains (38) and were upregulated
178 about 4-fold. Cell wall amidases cleave the amide bond that links stem peptides to N-acetylglucosamine
179 in PG glycan strands (39). CD630_36010 (4-fold induced) is a predicted D-alanyl-D-alanine
180 carboxypeptidase that removes the terminal D-Ala moiety from peptidoglycan pentapeptide sidechains.
181 This might limit 4-3 crosslinking of stem peptides, but could favor 3-3 crosslinking. Two proteins of
182 unknown function were upregulated >10-fold, CD630_07390 and CD630_07380. We suspect both of
183 these proteins are involved in PG metabolism because they are predicted to be exported and also
184 induced by lysozyme (40). Notable among the repressed genes in Wal-ON cells is *cd630_27680*, which
185 is down regulated about 4-fold and predicted to encode a cell wall hydrolase from the NlpC/P60 family,
186 a domain common to endopeptidases (39). Interestingly, this gene is preceded by two putative WalR

187 binding sites, and it has also been characterized as a sortase substrate (41). Another predicted PG
188 hydrolase, CD630_23880, is mildly repressed (~3-fold). Interestingly, this gene is cotranscribed with an
189 uncharacterized BlaI-BlaR regulatory system, *cd630_23890* and *cd630_23900*. Some BlaIR regulatory
190 systems respond to beta-lactam stress (42, 43).

191 One of the questions that motivated this study was whether the WalR system regulates genes for
192 S-layer proteins in *C. difficile*. Indeed, the Wal-ON regulon includes six S-layer protein genes, all of which
193 are upregulated by WalR: *cwp2*, *5*, *12*, *16*, *17* and *66*. Two of these genes were mentioned already, the
194 cell wall amidases *cwp16* and *cwp17*. The remaining four are of unknown function, although *cwp2* and
195 *cwp12* have domains implicated in adhesion or pathogenesis, and studies with *cwp66* have linked it to
196 adhesion (38). WalRK has been suggested to regulate an S-layer gene in *Bacillus anthracis* (44).

197

198 **Expression profiling under Wal-OFF conditions.** As a complementary approach to identify genes in
199 the WalR regulon, we assessed the effect of CRISPRi knockdown of the *wal* operon on global gene
200 expression. To this end, we performed RNA-seq on a 630Δerm derivative that has the CRISPRi
201 machinery (P_{xyl}::*dCas9*, P_{gdh}::*sgRNA-walA1*) integrated into the chromosome at *pyrE*. The control strain
202 was identical except that it expressed an innocuous sgRNA that does not target anywhere in the *C.*
203 *difficile* genome (P_{gdh}::*sgRNA*-neg). Two induction conditions were used. One of these, called "no xylose",
204 relied on leaky expression of *dCas9*. For this, overnight cultures were diluted into fresh TY to a starting
205 OD_{600} = 0.03 and harvested when they reached OD_{600} ~0.7 (Fig. S4C). For the other condition, called
206 "low xylose", cultures in exponential growth where induced with 0.1% xylose at an OD_{600} = 0.1 and
207 incubated 2.5 hours (~2 mass doublings) before harvest. This induction regime reduced cell density only
208 modestly (Fig. S4D).

209 There are 49 genes, organized in 27 operons that shift 4-fold or more under Wal-OFF conditions
210 (Table 3). The 27 operons contain an additional 14 genes that did not meet our 4-fold cut-off, all but three
211 of which nevertheless trended in the right direction. The three exceptions include a pseudogene
212 (*cd630_05260*) that is not detected by our RNA-seq analysis tool and two membrane proteins

213 (*cd630_05290* and *05280*) whose expression was unchanged. Thus, for the purposes of this analysis,
214 CRISPRi knockdown of the *wal* operon changed the expression of 60 genes, of which 44 were induced
215 and 16 were repressed. Curiously, for most of these genes the fold-change was larger in the absence of
216 xylose, suggesting that many of the effects on gene expression might be indirect.

217 The CRISPRi guide targets the first gene in the operon, *walA*, which was repressed 6.8-fold in
218 the absence of xylose and 35-fold with low xylose. As expected, polarity resulted in repression of the
219 downstream genes as well, ~5-fold with leaky CRISPRi, increasing to ~15-fold with low xylose. The
220 observed polarity confirms the predicted operon structure, including that a seemingly unrelated (and
221 according to Tn-seq nonessential) gene for a tRNA modification enzyme is indeed part of the operon.

222 Unexpectedly, the Wal-OFF gene set comprises mostly transporters and genes for various
223 metabolic functions. Not counting the members of the *wal* operon, only one of the genes is predicted to
224 be exported and 15 genes (25%) to be membrane proteins, a percentage comparable to the genome as
225 a whole (Methods). Remarkably, the Wal-OFF regulon does not include a single annotated PG
226 metabolism gene. However, we observed ~5-fold repression of the *dltDABC* operon, which is responsible
227 for the addition of D-alanine to teichoic acids (45). We identified a predicted WalR binding site
228 immediately upstream of *dltDABC*, suggesting direct regulation by WalR. This putative WalR binding site
229 had previously been recognized as one of two direct repeat sequences in the *dlt* promoter region ((45),
230 Table S4). D-alanylation of teichoic acids affects PG hydrolase activity (46, 47) and vancomycin
231 resistance in some bacteria (48, 49). In *C. difficile*, a *dltD* insertion mutant is sensitized to vancomycin
232 and some antimicrobial peptides, but the effects are <2-fold (48). Only one gene in Table 3 codes for an
233 S-layer protein—the hemagglutinin/adhesin *cwpV*, which was ~16-fold induced in no xylose. But this
234 gene is subject to phase variation (50), leading us to suspect it may not be a true member of the WalR
235 regulon.

236

237 **Comparison of the Wal-ON and the Wal-OFF gene sets reveals little overlap but opposing trends.**
238 There are only two proteins common to the Wal-ON and the Wal-OFF gene sets, *cd630_20160*

239 (hypothetical protein) and *cd630_28620* (annotated as a membrane peptidase). However, a large fraction
240 of the 79 Wal-ON genes that met the 4-fold cut-off trend in the opposite direction when evaluated under
241 Wal-OFF conditions, even though the magnitude of change is not as large (Fig. 5A, Table 2). A similar
242 observation was made when genes affected 4-fold or more under Wal-OFF conditions were examined
243 under Wal-ON conditions (Fig. 5B, Table 3).
244
245 **Select members of the WalR regulon were confirmed by plasmid-based reporter fusions**. To
246 confirm results of the RNA-seq analysis, we constructed *rfp* transcriptional fusions (51) to the promoter
247 regions for seven genes from the Wal-ON or Wal-OFF gene sets. Four genes were chosen primarily
248 because they were highly-induced when WalR was overexpressed: *cd630_07390*, *pgdA*, *cd630_07380*,
249 and *cd630_08670* (Table 2). Additional considerations included that *pgdA* has an obvious connection to
250 PG biogenesis (33, 34), while *cd630_08670* has a predicted WalR-binding site (Table S4). Two genes
251 were chosen because they were the most strongly repressed upon CRISPRi knockdown of the *wal*
252 operon and are preceded by a predicted WalR-binding site: *cd630_28620* and *cd630_05300* (Tables 3,
253 S4). In addition, *cd630_28620* is one of only two genes that made the 4-fold cut-off in both Wal-ON and
254 Wal-OFF conditions. The final gene chosen for confirmation with an *rfp* reporter was *dltD*, which
255 incorporates D-alanine into teichoic acids (45) and was modestly downregulated by CRISPRi knockdown
256 of the *wal* operon. *dltD* stood out because it has a predicted WalR-binding site and is one of the few cell
257 envelope-associated genes that was at least 4-fold repressed in Wal-OFF conditions (Tables 3, S4).
258 Reporter plasmids were constructed by PCR-amplifying ~300 bp upstream of the start codon for
259 each selected gene. These fragments contain transcriptional start sites for five of the seven genes (Clost-
260 Path database (52)); start sites for the remaining two genes have not been mapped. The PCR products
261 were cloned into an RFP reporter plasmid. The resulting plasmids were conjugated into the appropriate
262 Wal-ON and Wal-OFF strain pairs: 630Δerm versus 630Δerm P_{xyl}*::walR* and 630Δerm with sgRNA-*walA1*
263 versus 630Δerm sgRNA-neg, respectively. Reporter strains were grown under the same conditions as
264 used for the RNA-seq experiments, except that the Wal-OFF condition was limited to growth in the

265 absence of xylose, i.e., assaying the effect of leaky dCas9 expression on the reporter gene. Harvested
266 cells were fixed and transferred to aerobic conditions to allow RFP to mature. Fluorescence was
267 quantified by flow cytometry.

268 We found that all RFP reporters responded in the expected direction when *walR* expression was
269 manipulated, thus confirming the RNA-seq results by an orthogonal method (Fig. 6). However, the fold
270 changes were uniformly about 4-fold greater by RNA-seq than by RFP fluorescence. The reasons for this
271 difference are not known. As an aside, having RNA-seq and RFP fluorescence data for the same genes
272 enabled us to show these are correlated, i.e., baseline RFP fluorescence was higher for genes that
273 returned more reads in RNA-seq experiments (Fig. S5A). This correlation was expected and further
274 indicates our RNA-seq data are robust.

275

276 **Altering the expression level of select regulon genes does not induce the *wal* reporter.** In *B.*
277 *subtilis*, the WalR regulon can be induced or repressed by manipulating expression of *walR*-regulated
278 genes involved in PG metabolism (11, 53). We therefore asked whether manipulating expression of *wal*
279 regulon genes in *C. difficile* would induce or repress expression of a chromosomal P_{cd630_07390}::*rfp*
280 reporter. The reporter was chosen because this promoter was highly induced in Wal-ON conditions as
281 determined by RNA-seq (38-fold) or a plasmid-based RFP reporter fusion (7-fold). The chromosomal
282 P_{cd630_07390}::*rfp* reporter was validated by confirming ~10-fold increased red fluorescence upon
283 overexpression of *walR* from a P_{xyl} plasmid (Fig. S5B). Next, we introduced a panel of plasmids that
284 allowed us to directly target 13 WalR regulon genes by overexpression and/or CRISPRi. These 13 genes
285 were chosen for various reasons including large fold-changes in expression, relevance to cell wall
286 biogenesis, and the presence of WalR binding sites (Table S3). Of note, the gene set included a putative
287 cell wall amidase and the predicted PG hydrolase with a NlpC/P60 domain. Unfortunately, neither
288 overexpression nor CRISPRi knockdown of the selected *wal* regulon genes altered expression of the
289 P_{cd630_07390}::*rfp* reporter. Further work will be needed to determine whether these negative results reflect
290 technical difficulties or more fundamental differences in Wal signaling between *B. subtilis* and *C. difficile*.

291

292 **Perturbation of select Wal regulon genes individually does not lead to any Wal-associated**
293 **phenotypic defects.** As noted above, one motivation for determining the Wal regulon was to identify
294 genes that contribute to Wal phenotypes. Recall that induction of P_{xyl}::*walR* decreases viability, causes
295 cells to become phase bright and reduces autolysis in buffer containing 0.01% Triton X-100 (Fig. 3). Two
296 of the most highly induced genes in Wal-ON conditions encode the hypothetical proteins CD630_07380
297 and CD630_07390. However, overproduction of these proteins from P_{xyl} plasmids did not result in any
298 obvious phenotypic changes (Fig. 7). Likewise, a CRISPRi plasmid with an sgRNA that targets
299 *cd630_27680* had no effects on growth, morphology or lysis (Fig. 7); this gene encodes PG hydrolase
300 with two predicted WalR-binding sites and is among the most strongly repressed genes in Wal-ON
301 conditions.

302 CRISPRi silencing of the *wal* operon is lethal, and the terminal phenotypes include lysis and loss
303 of rod shape as reflected by an abundance of curved cells (Fig. 2). However, none of these phenotypes
304 were observed when we used a P_{xyl}::*cwpV* plasmid to overexpress the most highly-induced gene from
305 the Wal-OFF RNA-seq data set, which we tested even though *cwpV* is subject to phase-variation and
306 might not be part of the WalR regulon. We also observed on effect when we used CRISPRi to knock
307 down expression of *dltD*, which was among the more strongly repressed Wal-OFF genes and is preceded
308 by a putative WalR binding site (Fig. 8). While not an exhaustive evaluation of all regulon members, our
309 findings suggest the phenotypic defects observed upon perturbation of the Wal system are cumulative in
310 nature rather than due to changes in expression of any single gene much like what has been observed
311 in *B. subtilis* and *S. aureus* (8-10, 12).

312

313 **Discussion**

314 In *C. difficile* the WalRK TCS is predicted to reside in a four gene operon: *walA-walR-walK-truA2*.
315 We altered expression of the WalRK regulon by complementary approaches: depleting *C. difficile* of

316 WalRK by CRISPRi knockdown of the entire operon, and overproduction of WalR under P_{xyl} control. RNA-
317 seq revealed the *wal* operon is not autoregulated in *C. difficile*, as evidenced by a lack of induction when
318 WalR (or $WalR^{D66E}$) was ectopically expressed from a P_{xyl} promoter. Wal operons are not autoregulated
319 in other Firmicutes either. RNA-seq also confirmed the genes constitute an operon, because CRISPRi
320 targeting *walA* resulted in roughly equivalent knockdown of the three downstream genes. Further studies
321 will be needed to establish the specific role of each gene in WalRK signaling. We suspect *walA* is a bona
322 fide part of the Wal system because all *wal* operons studied to date include accessory genes for
323 membrane proteins that modulate WalK signaling (8, 10). But a rationale for why a non-essential tRNA
324 modification enzyme, *truA2,* should have come to reside in the *wal* operon is not obvious. This might be
325 the result of evolutionary happenstance.

326 As expected, extensive knockdown of the *wal* operon with CRISPRi or strong overproduction of
327 WalR from a P_{xyl} plasmid were both lethal. Phenotypic defects depended on how *walRK* expression was
328 manipulated, but included elongation, loss of rod shape (curved or wavy cells), phase bright cells,
329 enhanced or reduced autolysis, and altered sensitivity to antibiotics that target PG synthesis. Similar
330 phenotypes have been observed upon manipulating Wal signaling in other organisms (2, 6, 7, 9, 10, 12,
331 17, 18). But there are some intriguing differences. In *B. subtilis*, where phosphorylated WalR promotes
332 elongation, artificial upregulation of the Wal system causes cells to become elongated while artificial
333 downregulation causes cells to become short (10, 18). In *C. difficile*, however, overexpression of WalR
334 from P_{xyl} had no obvious effect on cell length while CRISPRi knockdown of the *wal* operon led to
335 elongation.

336 Vancomycin resistance presents another example of an inverse phenotype. In *S. aureus* down
337 regulating *walRK* expression increases resistance to vancomycin while up regulation of *walRK* decreases
338 vancomycin resistance (54, 55). Vancomycin-intermediate *S. aureus* (VISA) strains, both laboratory
339 derived (56) or isolated in the clinic (57), often have mutations in *walR* or *walK* that down regulate the
340 system (58). In contrast, we found that partial CRISPRi knockdown of the *wal* operon in *C. difficile* had

341 the opposite effect, namely, a modest increase in sensitivity to vancomycin. Vancomycin is a front line
342 treatment for *C. difficile* infections, so our findings suggest a small molecule that interferes with Wal
343 signaling might enhance the efficacy of vancomycin therapy.

344 RNA-seq identified over 150 genes whose expression responds to manipulation of Wal signaling
345 in *C. difficile*. Although this gene set is diverse, there are themes: many cell envelope proteins, many
346 hypotheticals, and about 10 proteins with various connections to PG metabolism. There are also 7 genes
347 for S-layer proteins, consistent with the need to coordinate S-layer assembly and remodeling with growth
348 and turnover of the PG sacculus. The PG hydrolases are of particular interest because they are prominent
349 members of the WalR regulon other Firmicutes (5, 12-16) and ectopic expression of one or more of these
350 enzymes can render *walRK* no longer essential regulators (6, 17, 18). In *C. difficile*, Wal-ON conditions
351 induced two putative cell wall amidases (*cwp16*, *cwp17*) and repressed one potential D,L-endopeptidase
352 (*cd630_27680*). Direct control of *cd630_27680* by WalR is suggested by the presence of two matches to
353 the WalR binding site consensus sequence about 100 nucleotides upstream of the start codon (Table
354 S4). The importance of these genes for any Wal-related phenotypes is unclear, however, because
355 overexpression and CRISPRi knockdown experiments did not result in any phenotypic changes or alter
356 expression of an RFP reporter that is induced under Wal-ON conditions. In addition to the putative
357 hydrolases, several genes in the WalR regulon may play a role in *controlling* PG hydrolase activity.
358 Deacetylation of PG N-acetylglucosamine (GlcNAc) (59), mDAP amidation (36), and D-alanylation of
359 teichoic acids (46, 47, 60, 61) have all been shown to affect hydrolase activity in other organisms.

360 *S. pneumoniae* is so far the only organism in which a single essential gene, the PG hydrolase
361 *pcsB*, has been identified to be responsible for the essentiality of the *wal* system (6, 7). In *B. subtilis*,
362 essentiality of the Wal system arises from the cumulative impact of aberrant expression of multiple genes
363 involved in turnover of PG (5, 10, 11). Wal essentiality is also polygenic in nature in *S. aureus* (8). This
364 seems to be the case in *C. difficile* as well. Although CRISPRi silencing of the *wal* operon leads to cell
365 lysis, the Wal-OFF gene set (Table 3) does not include any genes determined to be essential by

366 transposon mutagenesis (27). In contrast, the Wal-ON regulon (Table 2) includes 3 essential genes. Two
367 of these are induced by WalR, DNA ligase (*ligA, cd630_33090*) and a putative Calcium-chelating protein
368 (*cd630_26810*); one is repressed, the PG precursor synthesis protein MurE (*cd630_26640*). It is possible
369 that repression of *murE* contributes to death during overexpression of WalR, but not during CRISPRi
370 knockdown of the *wal* operon, because *murE* expression did not change under that condition. Overall,
371 our findings suggest essentiality of WalRK is driven by a deleterious imbalance of multiple processes.
372 (As an aside, it is worth noting that repression of *murE* under Wal-ON conditions is not what one would
373 expect if WalR promotes increased PG synthesis, as in other *B. subtilis* (11, 53)).

374 Here we have provided an initial delineation of Wal phenotypes and the WalR regulon in *C.*
375 *difficile*. Our findings raise a number of exciting questions. Is the protein WalA involved in WalRK
376 signaling, and if so, how? What signals are sensed by WalK? Of note, owing to differences in crosslinking
377 (23), the PG hydrolysis products implicated in regulating WalK activity in *B. subtilis* (11) are not very
378 abundant in *C. difficile*. Moreover, *C. difficile* WalK is missing an intracellular PAS domain found in most
379 other WalK proteins, suggesting *C. difficile* WalK senses different signals and/or transmits those signals
380 differently. Another open question is which WalR regulon genes are controlled directly by WalR. It will
381 also be important to determine the functions of the WalR regulated genes, especially the many
382 hypothetical proteins. Answers to these questions are likely to provide novel insights into cell wall
383 biogenesis and might point the way towards improved therapies against this important pathogen.

384

385 **Methods**

386 **Strains, media, and growth conditions.** Bacterial strains are listed in Table 4. *C. difficile* strains used
387 in this study were derived from either 630Δerm or R20291, both of which have been sequenced. *C.*
388 *difficile* was routinely grown in tryptone-yeast extract (TY) medium, supplemented as needed with
389 thiamphenicol at 10 µg/ml (TY-Thi). TY medium consisted of 3% tryptone, 2% yeast extract, and 2% agar

390 (for plates). Brian heart infusion (BHI) media was prepared per manufacturer's (DIFCO) instructions. *C.*
391 *difficile* strains were maintained at 37°C in an anaerobic chamber (Coy Laboratory Products) in an
392 atmosphere of 10% H_2, 5% CO_2, and 85% N_2. *Escherichia coli* strains were grown in LB medium at 37°C
393 with chloramphenicol at 10 µg/ml or ampicillin at 100 µg/ml as needed. LB medium contained 1%
394 tryptone, 0.5% yeast extract, 0.5% NaCl, and 1.5% agar (for plates). OD_{600} measurements were made
395 with the WPA Biowave CO8000 tube reader in the anaerobic chamber.
396
397 **Plasmid and strain construction**. All plasmids are listed in Table 5; an expanded version of this table
398 which includes additional information relevant to plasmid assembly is provided in Table S2A in the
399 supplemental material. Plasmids were constructed by isothermal assembly (62) using reagents from New
400 England Biolabs (Ipswich, MA). Regions of plasmids constructed using PCR were verified by DNA
401 sequencing. The oligonucleotide primers used in this work were synthesized by Integrated DNA
402 Technologies (Coralville, IA) and are listed in Table S2B. All plasmids were propagated using OmniMax
403 2-T1R as the cloning host, transformed into HB101/pRK24 (63, 64), and then introduced into *C. difficile*
404 strains by conjugation. Chromosomal fusions at the *pyrE* locus in 630Δerm were constructed by allelic
405 exchange (29) using *C. difficile* CRG1496 (630Δ*erm* Δ*pyrE*) as a *pyrE*-deficient recipient. The allelic
406 exchange restored a functional *pyrE* gene.
407
408 **Conjugation into *C. difficile.*** Our experiments required conjugating plasmids into *C. difficile*
409 strains R20291 and 630Δerm. In the case of R20291 we encountered problems with low conjugation
410 efficiencies even with heat shock as described (65). After testing several modifications of the procedure,
411 we found that performing conjugations on filters reliably increased efficiency more than 10-fold (Fig. S6).
412 We now routinely use filters for all our conjugations. Briefly, the *E. coli* donor strain (an HB101/pRK24
413 derivative harboring the cargo plasmid) was grown overnight in LB Amp^{100} Cam^{10}. The donor strain was
414 collected gently by centrifugation of a 0.5 ml aliquot at 5000 x g for 1 min, then washed with 1 ml TY and
415 pelleted again. The washed cell pellet was moved into the anaerobic chamber. R20291 was prepared for

416 conjugation by a heat shock step (65). For this, a 200 µl aliquot of the overnight culture of the R20291
417 recipient was transferred to a 1.5 ml microfuge tube and incubated at 48°C for 5 min in a Fisherbrand
418 Dry bath (with water-filled wells). Then 100 µl of heat-shocked R20291 was used to take up the pellet of
419 *E. coli* donor cells. The strain mixture was then pipetted on to a 25 mm diameter, 0.45 µm pore size
420 Millipore mixed cellulose filter (HAWP02500) placed on brain heart infusion (BHI) plates. After incubation
421 for 24 h at 37°C, cells were flushed from the membrane with 500 µL TY and 200-500 µL of the resulting
422 bacterial slurry was plated on TY amended with thiamphenicol (10 µg/ml), kanamycin (50 µg/ml) and
423 cefoxitin (8 µg/ml) to select for exconjugants. Conjugations into 630Δerm were done identically except
424 the heat shock step was omitted.
425
426 **Viability assay.** The effect of CRISPRi silencing on plating efficiency was evaluated by making a 10-fold
427 serial dilution of a culture grown overnight in TY Thi10 and spotting 5 µl of each dilution on TY Thi10 agar
428 with and without 1% xylose. Plates were photographed after overnight incubation (~18 h).
429
430 **Microscopy.** Cells were immobilized using thin agarose pads (1%). Phase-contrast micrographs were
431 recorded on an Olympus BX60 microscope equipped with a 100× UPlanApo objective (numerical
432 aperture, 1.35). Micrographs were captured with a Hamamatsu Orca Flash 4.0 V2+ complementary metal
433 oxide semiconductor (CMOS) camera. The image analysis tool MicrobeJ (66) was used to measure cell
434 length and sinuosity, which is the length of the cell axis divided by the distance between the poles. A
435 perfectly straight rod has a sinuosity value of 1, while a curved or wavy cell has a larger value. We
436 classified cells as curved if their sinuosity was ≥1.03 (see Fig. S2 for examples).
437
438 **Fixation protocol.** A 500-µl aliquot of cells in growth medium was added directly to a microcentrifuge
439 tube containing 120 µl of a 5x fixation cocktail: 100 µl of a 16% (wt/vol) paraformaldehyde aqueous
440 solution (Alfa Aesar, Ward Hill, MA) and 20 µl of 1 M $NaPO_4$ buffer (pH 7.4). The sample was mixed,
441 incubated in the anaerobic chamber at 37°C for 30 min, then on ice 30 min, and removed from the

442 chamber. The fixed cells were washed twice with 1 mL phosphate-buffered saline (PBS), resuspended
443 in 50 µl of PBS, and left in the dark for 18 h to allow for chromophore maturation.
444
445 **MIC determination.** Antibiotic sensitivity was determined in 96 well plates. A twofold dilution series of
446 select antibiotics was prepared in 50 µl TY medium. Wells were then inoculated with 50 µl of a diluted
447 culture suspension (10^6 CFU/ml; calculated OD_{600} ~0.005). Plates were imaged and evaluated after 17h
448 at 37°C.
449
450 **Lysis assay.** Cell cultures (1 mL) were removed from the anaerobic chamber, pelleted and resuspended
451 in 700 µL 0.01% Triton X-100 in 50 mM $NaPO_4$ buffer (pH 7.4). Of this 700 µL, three 200 µL replicates
452 were pipetted into wells of a clear, flat bottom 96-well plate. The turbidity was measured at 600 nm every
453 15 min for 10 h in a plate reader (Tecan Infinite M200 Pro).
454
455 **Flow cytometry.** Cells were analyzed at the Flow Cytometry Facility at the University of Iowa using the
456 Becton, Dickinson LSR II instrument with a 561-nm laser, a 610/20-nm-band-pass filter, and a 600 LP
457 dichroic filter. Data were analyzed using BD FACSDiva software.
458
459 **Culture growth for RNA-seq samples**. To achieve robust, quality data all experiments were performed
460 on three different days for biological replicates. Cultures were grown in 100 mL TY as follows. Wal-ON:
461 to characterize the effect of overexpressing *walR*, strains were subcultured to OD_{600} ~0.05, grown to 0.2,
462 induced with xylose to 3% and grown for an additional 3h (Fig. S4A). Wal-OFF: to characterize the effect
463 of partial knockdown of the *wal* operon under leaky CRISPRi conditions, strains were subcultured to
464 OD_{600} ~0.03 and grown to ~0.7 before harvesting (Fig. S4C). To test the effect of stronger knockdown of
465 the *wal* operon, growth conditions were identified that allowed exposing cells to moderate levels of xylose
466 (0.1%) without a significant loss of biomass. Strains were subcultured to OD_{600} ~0.03, grown to 0.3,
467 diluted back to ~0.1 and induced with xylose to a final concentration of 0.1% and harvested after an

468 additional 2.5 h of growth (Fig. S4D). From each condition, 25 mL culture was fixed by rapidly mixing with
469 25 mL ice-cold 1:1 ethanol:acetone that had been brought into the anaerobic chamber on dry ice. Fixed
470 cells were stored at -80°C until further workup.
471
472 **RNA isolation and RNA-Seq.** Fixed culture samples were thawed, pelleted for 10 min at 8000 x g, 4°C
473 and pellets washed once with 500 µL 1% β-mercaptoethanol (β-ME) in water. Subsequent steps are an
474 adaptation of the Qiagen RNeasy Mini Kit procedure. The washed pellet was resuspended in 1 mL of the
475 Qiagen-provided RTL buffer amended with 1% β-ME and transferred to a 2 mL screwcap tube filled with
476 glass beads (0.1 mm diameter) to a height of ~2-3 mm. Cells were lysed with the FastPrep-24
477 homogenizer with two cycles at 6m/s for 45 s, resting on ice for 3 min between cycles. The homogenized
478 material was pelleted at 14,000 x g for 15 min at 4°C. The supernatant was removed, adjusted to 900 µL
479 with RTL/β-ME, mixed with 500 µL ethanol and loaded onto the Qiagen RNeasy spin column. Subsequent
480 steps followed the manufacturer's protocol. The RNA was eluted with 50 µL water and DNase treated
481 twice (Ambion Turbo DNA-free). Absence of DNA was evaluated by amplifying a 364 bp region of *mldA*
482 with Taq DNA polymerase for 30 cycles. The RNA integrity number (RIN) was determined with an Agilent
483 Bioanalyzer at the Iowa Institute for Human Genetics, Genomics Division. All samples had a RIN of 9.4
484 or higher. Typical yields from 25 mL culture were 8-20 µg RNA at 200-500 ng/µL.
485 RNA samples were submitted to the Microbial Genome Sequencing Center (MiGS) in Pittsburgh,
486 PA. MiGS performed Illumina Stranded RNA library preparation paired with RiboZero Plus (per
487 manufacturer's specifications) and sequenced on a NextSeq 500 using a 75cyc High Output flowcell.
488 Fastq files were trimmed and filtered using a combination of Trimmomatic (67) and FastQC
489 (https://www.bioinformatics.babraham.ac.uk/projects/fastqc/). Alignment, normalization and differential
490 expression was analyzed with SeqMan NGen® Version 17.2. DNASTAR, Madison, WI. Annotation was
491 imported from NCBI with additional information obtained from progenomes (68). All subsequent analysis
492 was performed in Excel and GraphPad Prism 9.
493

494 **Bioinformatics**. Gene sequences and operon organization were obtained from the BioCyc data
495 collection (32, 69). SignalP 5.0 (70) was used to search for Type I and Type II signal peptides. BUSCA
496 (71) was used to predict protein cellular location. When all *C. difficile* proteins were run through the
497 prediction programs, SignalP predicted ~7% to be exported. BUSCA predicted ~4% to exported and
498 ~25% to be membrane associated. Cell wall association in Tables 2 and 3 was reported as follows: (i)
499 signal peptidase substrate if predicted by SignalP; (ii) for all remaining genes: membrane protein if
500 predicted by BUSCA.

501 Putative WalR binding sites were identified with Virtual Footprint (72) by querying with (1) the *B.*
502 *subtilis* consensus motif, TGTWAH-N5-TGTWAH (14), (2) the same motif, but allowing one mismatch, or
503 (3) TGTNDH-N5-BKBWRN (8). Searches were limited to the intergenic region of the genome and
504 generated 29, 522, and 684 hits respectively.

505

506 **Acknowledgements**

507 This work was supported by National Institutes of Health grants R01AI087834 (CDE) and
508 R01AI155492 (CDE and DSW) from the National Institutes for Allergy and Infectious Disease. Cell
509 fluorescence was quantitated at the Flow Cytometry Facility, which is a Carver College of Medicine /
510 Holden Comprehensive Cancer Center core research facility at the University of Iowa. The facility is
511 funded through user fees and the generous financial support of the Carver College of Medicine, Holden
512 Comprehensive Cancer Center, and Iowa City Veteran's Administration Medical Center. RNA integrity
513 was characterized by the Genomics Division of the Iowa Institute of Human Genetics which is supported,
514 in part, by the University of Iowa Carver College of Medicine. We thank Nigel Minton for pMTL-YN1C,
515 Brianne Zbylicki for plasmid pBZ101, and members of the Ellermeier and Weiss laboratories for helpful
516 discussions.

517

518 **Table 1.** Effect of CRISPRi-silencing *wal* on sensitivity to antibiotics[a]

	MIC [µg/mL]		
	sgRNA-neg	sgRNA-*walA1*	sgRNA-*walA2*
Ampicillin	6.3	3.5	3.1
Imipenem	3.1	3.1	2.6
Vancomycin	4.6	0.9	0.7
Daptomycin	11.3	4.1	5.7
Bacitracin	250	250	250
Novobiocin	13	17	16

519 [a]Results are the average of measurements done in duplicate on four different days.

520 **Table 2. Genes affected by Wal-ON conditions.**

521

Gene, changed ≥ 4-fold	Operon[1]	Gene name	Annotation	Log$_2$ fold change			Cell wall association[3]
				WalR overexpression		CRISPRi against *wal*[2]	
				WalR	WalR^{D66E}		
cd630_07390	07390		hypothetical protein	5.26	5.70	-1.38	SPI
cd630_15220	15220	*pgdA*	peptidoglycan deacetylase	4.02	4.26	-1.09	SPI
cd630_05490	05490		hypothetical protein	3.87	4.51	-1.84	SPI
	17810	*walA*	lipoprotein	nc[4]	nc	-2.76	SPII
cd630_17820	17820	*walR*	TC response regulator	3.81	3.67	-2.51	
	17830	*walK*	TC sensor histidine kinase	nc	nc	-2.33	Membrane
	17840	*truA2*	tRNA pseudouridine synthase A	nc	nc	-2.34	
cd630_07380	07380		hypothetical protein	3.43	4.14	-1.22	SPI
cd630_08670	08670		hypothetical protein	3.28	3.97	nc	Membrane
cd630_07400	07400		PLP dependent aminotransferase	3.21	2.38	nc	
cd630_10880	10880		hypothetical protein	2.88	3.14	-1.40	Membrane
cd630_01660	01660		peptidase	2.76	2.95	nc	
	01650		amino acid transporter	nc	nc	nc	Membrane
cd630_27940	27940	*cwp12*	cell wall binding protein	2.69	2.82	nc	SPI
cd630_33090	33090	*ligA*	DNA ligase	2.64	2.62	nc	
cd630_18250	18250	*metY*	O-acetylhomoserine sulfhydrylase	2.50	2.80	-0.57	
cd630_18260	18260	*metA*	homoserine O-succinyltransferase	2.60	2.85	-0.88	
cd630_14281	14281		hypothetical protein	2.59	3.22	nc	
cd630_27860	27860	*cwp5*	cell wall binding protein	2.51	2.65	nc	SPI
cd630_25380	25380		lipoprotein	2.47	2.70	-0.70	SPII
cd630_03910	03910	*asnB*	asparagine synthetase	2.47	3.30	nc	Membrane
cd630_14960	14960		hypothetical protein	2.37	2.86	-0.74	SPI
cd630_25370	25370		5'-nucleotidase/phosphoesterase	2.33	2.49	-0.59	SPI
cd630_27910	27910	*cwp2*	cell wall binding protein	2.30	2.36	-0.59	SPI
	27900		LmbE-like deacetylase	1.56	1.46	-0.55	
	27890	*cwp66*	cell wall binding protein	1.41	1.42	-0.58	SPI
cd630_28620	28620		peptidase	2.29	2.24	-2.53	
cd630_34880	34880	*gtaB1*	UTP-G1P uridylyltransferase	2.23	2.34	-0.73	
cd630_20580	20580		hypothetical protein	2.22	2.43	-1.26	Membrane
cd630_07410	07410	*glpK1*	glycerol kinase	2.21	0.63	nc	
	07420	*eutH*	ethanolamine utilization protein	1.46	nc	nc	Membrane
	10350	*cwp16*	amidase, cell wall binding protein	1.24	1.33	nc	SPI
cd630_10360	10360	*cwp17*	amidase, cell wall binding protein	2.15	2.35	nc	SPI
cd630_21170	21170	*trxB2*	thioredoxin reductase	2.12	2.18	nc	
cd630_00210	00210	*pycA*	pyruvate carboxylase	2.10	2.16	-0.46	
cd630_13890	13890		chloromuconate cycloisomerase	2.09	2.18	-0.28	
	13900		hypothetical protein	1.30	1.64		Membrane
cd630_22490	22490		ATPase	2.07	2.20	nc	

Gene, changed ≥ 4-fold	Operon[1]	Gene name	Annotation	Log$_2$ fold change			Cell wall association[3]
				WalR overexpression		CRISPRi against *wal*[2]	
				WalR	WalR^{D66E}		
cd630_22480	22480		hypothetical protein	1.81	2.04	nc	
cd630_10890	10890	*rgbR*	TC response regulator	2.04	2.24	-1.13	
	10900	*rgbS*	TC sensor HK (fragment)	nc	1.16	nc	Membrane
cd630_30930	30930		aminobutyrate hydrolase	2.15	2.35	nc	
	30920		putative amino acid transporter	1.52	1.02	nc	Membrane
cd630_26810	26810		putat. Ca-chelating protein	2.01	2.59	nc	SPI
cd630_36010	36010		D-Alanyl-D-alanine carboxypeptidase	1.99	2.35	-1.38	SPI
cd630_00220	00220		Elongation factor G	1.97	2.09	nc	
cd630_14290	14290		Acyl-CoA N-acyltransferase	1.92	2.47	-1.15	
cd630_22280	22280		Hypothetical protein	1.83	2.05	-0.70	Membrane
cd630_01100	01100		Hypothetical protein	1.81	2.02	nc	Membrane
	01110		Hypothetical protein	1.51	1.73	nc	SPI
	01111		Hypothetical protein	nc	1.14	nc	
cd630_09940	09940		Serine-pyruvate aminotransferase	1.77	2.10	nc	
cd630_19942	19942		Hypothetical protein	1.74	2.12	nc	
cd630_05270	05270		Beta-lactamase-like hydrolase	1.73	2.13	-0.85	
cd630_22270	22270		Radical SAM protein	1.67	2.02	-0.55	SPII
cd630_18070	18070		NADPH-dependent FMN reductase	1.49	2.07	-1.53	Membrane
cd630_03901	03901		Hypothetical protein	0.92	2.37	nc	
cd630_10631	10631		Hypothetical protein	-0.07	2.18	-0.62	Membrane
cd630_30360	30360		Major facilitator superfamily transporter	-1.59	-2.13	1.11	Membrane
cd630_10540	10540	*bcd2*	Acyl-CoA dehydrogenase	-1.93	-2.23	1.03	
cd630_10550	10550	*etfB*	Electron transfer flavoprotein beta	-1.78	-2.11	1.07	
cd630_10560	10560	*etfA*	Electron transfer flavoprotein alpha	-1.95	-2.18	1.10	
cd630_10570	10570	*crt2*	3-Hydroxybutyryl-CoA dehydratase	-1.96	-2.27	1.06	
cd630_31000	31000		C4-dicarboxylate anaerobic carrier	-1.88	-2.59	nc	Membrane
cd630_30990	30990		Amidohydrolase	-1.80	-2.47	nc	Membrane
cd630_10580	10580	*hbd*	3-Hydroxybutyryl-CoA dehydrogenase	-1.86	-2.05	0.89	SPII
cd630_10590	10590	*thlA1*	Acetyl-CoA acetyltransferase	-1.96	-2.16	0.77	
	16820	*queK*	Queuosine hydrolase monomer	-1.31	-1.60	nc	
	16830		ECF transporter S-comp.	-1.39	-1.65	nc	Membrane
cd630_16840	16840	*queL*	Radical SAM superfamily protein	-1.90	-2.06	nc	
	23900		BlaI-like	-1.47	-1.65	nc	
cd630_23890	23890		BlaR-like	-1.94	-2.26	0.80	Membrane
	23880		Putat. PG hydrolase	-1.50	-1.77	nc	SPI
	36040		Hypothetical protein	-0.86	-0.94	0.71	
cd630_36030	36030		Phosphoesterase	-1.97	-2.01	1.09	Membrane
cd630_14040	14040		Oligopeptide transporter	-2.02	-2.03	nc	Membrane
	14041		Hypothetical protein	-2.02	-1.88	nc	
	25120		PTS, subunit IIA	-1.11	-1.47	nc	
	25110		PTS, antiterminator	-1.45	-1.46	nc	
cd630_25100	25100		PTS, subunit IIBC	-2.04	-2.19	0.97	Membrane

Gene, changed ≥ 4-fold	Operon[1]	Gene name	Annotation	Log$_2$ fold change			Cell wall association[3]
				WalR overexpression		CRISPRi against *wal*[2]	
				WalR	WalR^{D66E}		
cd630_25320	25320		Alanine-glyoxylate transaminase	-2.05	-2.34	1.41	
cd630_25310	25310		Hypothetical protein	-2.67	-2.75	1.35	Membrane
cd630_27680	27680		Cell-wall hydrolase	-2.06	-2.29	nc	SPI
cd630_29660	29660	*adhE1*	Acetaldehyde-CoA/alcohol dehydrogenase	-2.08	-2.37	-1.09	Membrane
cd630_18120	18120		Response regulator	-2.08	-2.28	nc	
cd630_22600	22600		Major facilitator superfamily transporter	-2.13	-2.32	nc	Membrane
cd630_20160	20160		Hypothetical protein	-2.19	-2.29	4.18	
cd630_25090	25090		Glycoside hydrolase	-2.22	-2.33	1.16	
cd630_21070	21070		Permease family protein	-2.23	-2.32	nc	Membrane
cd630_10220	10220		YczE-like membrane protein	-2.26	-2.73	0.93	Membrane
	10230		Transcriptional regulator	-1.70	-1.94	1.63	
cd630_10240	10240	*potA*	ABC transport ATP-binding protein	-2.27	-2.36	1.77	
cd630_10250	10250	*potB*	ABC transport permease	-2.47	-2.82	1.72	Membrane
cd630_10260	10260	*potC*	ABC transport permease	-2.53	-2.39	1.60	Membrane
cd630_10270	10270	*potD*	ABC transport substrate binding protein	-2.29	-2.37	1.55	SPII
cd630_26640	26640	*murE*	UDP-N-acetylmuramoylalanyl-D-glutamate-2, 6-diaminopimelate ligase	-2.85	-3.07	0.93	
cd630_26670	26670	*ptsG-BC*	PTS, subunit IIBC	-3.17	-3.52	nc	SPI
cd630_26660	26660	*ptsG-A*	PTS, subunit IIA	-3.12	-3.51	nc	
cd630_21510	21510		Hypothetical protein	-3.56	-3.82	0.68	Membrane

[1] Lists other operon members in order

[2] CRISPRi against *wal*: Fold change comparing sgRNA-neg to sgRNA-*walA1* strain in the absence of xylose

[3] Reports predictions by SignalP (SPI, predicted to be a substrate of signal peptidase I; SPII, predicted to be a substrate of signal peptidase II) and by BUSCA (membrane). The BUSCA prediction is only given for those genes that were not already predicted to be SPI or SPII substrates by SignalP.

[4] nc: no change, i.e. the fold change was close to 1 and the P-value >0.05

Abbreviations: TC (two component), PTS (phosphoenolpyruvate-dependent sugar phosphotransferase system)

532 **Table 3** Genes affected by Wal-OFF conditions

533

Gene, changed ≥ 4-fold	Operon[1]	Gene name	Annotation	Log$_2$ fold change			Cell wall association[3]
				CRISPRi		WalR OE[2]	
				No xyl	Low xyl		
cd630_05140	05140	*cwpV*	Hemagglutinin/adhesin	4.69	2.74	nc[4]	SPI
cd630_20160	20160		Hypothetical protein	4.18	1.65	-2.19	
cd630_11700	11700		Hypothetical protein	3.52	1.83	nc	
cd630_11710	11710	*etfB4*	Electron transfer flavoprotein alpha	3.30	1.40	nc	
cd630_11720	11720	*etfA4*	Electron transfer flavoprotein alpha	2.58	1.24	nc	
cd630_11730	11730		FAD-linked oxidase	2.17	1.08	nc	
cd630_08320	08320	*aksA*	Trans-homoaconitate synthase	3.11	2.02	nc	
cd630_08330	08330	*acnB*	Aconitate hydratase	3.06	2.05	nc	
cd630_08340	08340	*icd*	Isocitrate dehydrogenase	3.07	2.16	nc	
cd630_17290	17290		Sodium:phosphate symporter	2.76	0.45	-1.46	Membrane
cd630_13840	13840		LamB/YcsF family protein	2.17	0.88	nc	
cd630_13850	13850		Hypothetical protein	2.36	1.15	nc	Membrane
cd630_13860	13860		Allophanate hydrolase subunit 1	2.52	1.28	nc	
cd630_13870	13870		Allophanate hydrolase subunit 2	2.60	1.14	nc	
cd630_24260	24260	*buk1*	Butyrate kinase	2.45	nc	-1.41	
	24250	*ptb2*	Phosphate butyryltransferase	1.65	nc		
cd630_24240	24240		Pyridoxal phosphate-dependent transferase	2.55	nc	-1.15	
	24230		Putative transporter	1.17	nc		Membrane
cd630_07650	07650	*srlEa*	PTS, IIB N-terminal component	2.17	nc	nc	
cd630_07660	07660	*srlEb*	PTS, IIB C-terminal component	2.29	nc	nc	Membrane
cd630_07670	07670	*srlB*	PTS, IIA subunit	2.27	nc	nc	
cd630_07680	07680	*srlD*	Sorbitol-6-phosphate dehydrogenase	2.35	nc	nc	
	00350		Transcriptional regulator	1.46	0.55	-0.86	
cd630_00360	00360	*acoA*	Acetoin dehydrogenase E1 alpha	2.20	0.94	nc	
cd630_00370	00370	*acoB*	Acetoin dehydrogenase E1 beta	2.29	0.91	nc	
cd630_00380	00380	*acoC*	Acetoin dehydrogenase E2	2.20	0.72	nc	
cd630_00390	00390	*acoL*	Acetoin dehydrogenase E3	2.04	0.83	-0.57	
cd630_30010	30010		Hydrolase/isomerase/hydratase	2.25	nc	nc	
cd630_23920	23920		tRNA-binding protein	2.15	1.65	-1.77	
cd630_30960	30960	*bglA3*	6-Phospho-beta-glucosidase	2.13	nc	nc	
cd630_30950	30950	*bglA2*	6-Phospho-beta-glucosidase	2.07	nc	nc	
cd630_25150	25150		Aspartate aminotransferase	2.12	2.38	-1.76	

Gene, changed ≥ 4-fold	Operon[1]	Gene name	Annotation	Log$_2$ fold change			Cell wall association[3]
				CRISPRi		WalR OE[2]	
				No xyl	Low xyl		
	24291		Flavo/ferredoxin oxidoreductase delta	1.19	nc	nc	
cd630_24290	24290		Flavo/ferredoxin oxidoreductase alpha	2.11	nc	-0.91	
	24280		Flavo/ferredoxin oxidoreductase beta	1.66	nc	nc	
	24270		Flavo/ferredoxin oxidoreductase gamma	1.50	nc	nc	
cd630_30040	30040	*kdgT2*	2-Keto-3-deoxygluconate permease	2.08	0.33	0.93	Membrane
cd630_30020	30020	*uxaA*	D-galactate dehydratase/altronate hydrolase	2.06	0.25	nc	
cd630_32630	32630	*pstC*	Phosphate ABC transporter, PstC	2.03	nc	nc	Membrane
	32620	*pstA*	Phosphate ABC transporter, PstA	1.03	nc	nc	Membrane
	32610	*pstB*	Phosphate ABC transporter, ATP binding	1.80	nc	nc	
	32600	*phoU*	Phosphate uptake regulator	1.25	nc	nx	
	30980	*bglG1*	PTS, antiterminator	0.95	nc	nc	
cd630_30970	30970	*bglF2*	PTS, subunit IIABC	2.01	nc	-0.76	Membrane
cd630_28540	28540	*dltD*	D-alanine transferase	-1.52	-2.41	1.03	Membrane
cd630_28530	28530	*dltA*	D-ala-D-ala carrier protein ligase 1	-1.34	-2.27	0.84	
cd630_28520	28520	*dltB*	D-alanyl transferase	-1.34	-2.23	0.49	Membrane
	28510	*dltC*	D-ala-D-ala carrier protein ligase 2	-1.27	-1.89	nc	
cd630_09000	09000	*opuCA*	ABC transporter ATP-binding protein	-1.69	-2.36	1.46	
cd630_09010	09010	*opuCC*	ABC transporter permease	-1.68	-2.40	1.27	Membrane
cd630_05190	05190		Hypothetical protein	-2.00	-2.59	0.57	Membrane
	05260		Aminobenzoyl-glutamate transporter	nd[5]	nd	nd	
cd630_05250	05250		Peptidase	-2.15	-1.08	nc	
cd630_17671	17671		Hypothetical protein	-2.18	-1.99	nc	
cd630_17680	17680		Membrane protein	-2.23	-2.18	0.56	Membrane
cd630_17810	17810	*walA*	Lipoprotein	-2.76	-5.14	nc	SPII
cd630_17820	17820	*walR*	TC response regulator	-2.51	-3.91	3.81	
cd630_17830	17830	*walK*	TC sensor histidine kinase	-2.33	-4.03	nc	Membrane
cd630_17840	17840	*truA2*	tRNA pseudouridine synthase A	-2.34	-3.92	nc	
cd630_05300	05300		Membrane protein	-2.47	nc	nc	Membrane
	05290		Membrane protein	nc	nc	nc	Membrane
	05280		Amidohydrolase	nc	nc	0.92	
cd630_28620	28620		Peptidase	-2.53	-1.43	2.29	

[1] Lists other operon members in order

[2] Fold change comparing WalR overexpression to negative control strain

537 [3] Predictions by SignalP (SPI, predicted to be a substrate of signal peptidase I; SPII, predicted to be a
538 substrate of signal peptidase II) and by BUSCA (membrane). The BUSCA prediction is only given for
539 those genes that were not already predicted to be SPI or SPII substrates by SignalP.
540 [4] nc: no change, i.e. the fold change was close to 1 and the P-value >0.05
541 [5] nd: CD630_05260 is a pseudogene that was not detected by the RNA-seq analysis tool
542 Abbreviations: TC (two component), PTS (phosphoenolpyruvate-dependent sugar phosphotransferase
543 system)
544

545 **Table 4** Strains used in this study

546

Strain	Genotype and/or description	Source or reference
E. coli		
OmniMAX-2 T1^R	F′ [*proAB*$^+$ *lacI*^{q} *lacZ*ΔM15 Tn*10*(Tet^R) Δ(*ccdAB*)] *mcrA* Δ(*mrr-hsdRMS-mcrBC*) φ80(*lacZ*)ΔM15 Δ(*lacZYA-argF*) *U169 endA1 recA1 supE44 thi-1 gyrA96 relA1 tonA panD*	Invitrogen
HB101/pRK24	F− *mcrB mrr hsdS20*(r_B^- m_B^-) *recA13 leuB6 ara-14 proA2 lacY1 galK2 xyl-5 mtl-1 rpsL20*	(63, 64)
C. difficile		
R20291	Wild-type *C. difficile strain* from UK outbreak (ribotype 027)	
630Δ*erm*	Spontaneous erythromycin-sensitive derivative of strain 630 (ribotype 012)	(73)
CRG1496	630Δ*erm*Δ*pyrE*	(29)
UM275	630Δ*erm* with P_{veg}::*rfp* downstream of *pyrE*	(26)
UM554	630Δ*erm* with P_{xyl}::*dCas9* P_{gdh}::*sgRNA-neg* downstream of *pyrE*	This study
UM555	630Δ*erm* with P_{xyl}::*dCas9* P_{gdh}::*sgRNA-cd630_17810-1* downstream of *pyrE*	This study
UM556	630Δ*erm* with P_{xyl}::*dCas9* P_{gdh}::*sgRNA-cd630_17810-2* downstream of *pyrE*	This study
UM626	630Δ*erm* with P_{xyl}::*walR* downstream of *pyrE*	This study
UM628	630Δ*erm* with P_{xyl}::*walR*^{D66E} downstream of *pyrE*	This study
UM926	630Δ*erm* with P_{cd630_0739}::*mCherryOpt* downstream of *pyrE*	This study

547

548

549 **Table 5.** Plasmids used in this study

550

Plasmid	Relevant features	Reference or comment
pAP114	P_{xyl}::*mCherryOpt catP*	(26)
pBZ101	P_{xyl} empty vector	This study
pCE636	P_{dltD}::*mCherryOpt catP*	This study
pCE738	P_{xyl}::*dCas9-opt* P_{gdh}::*sgRNA-dltD-1 catP*	(34)
pCE691	P_{xyl}::*walR catP*	This study
pCE738	P_{xyl}::*dCas9-opt* P_{gdh}::*sgRNA-dltD-1 catP*	(34)
pCE741	P_{xyl}::*cdr2656*	This study
pCE744	P_{xyl}::*dCas9-opt* P_{gdh}::*sgRNA-cd630_27680-1 catP*	This study
pCE745	P_{xyl}::*dCas9-opt* P_{gdh}::*sgRNA-cd630_27680-2 catP*	This study
pCE789	P_{xyl}::*dCas9-opt* P_{gdh}::*cwpV-1 catP*	This study
pCE791	P_{xyl}::*cwpV*	This study
pDSW1728	P_{tet}::*mCherryOpt catP*	(51)
pDSW2037	P_{xyl} in integration vector pMTL-YN1C *catP*	This study
pDSW2053	P_{xyl}::*dCas9opt-*P_{gdh}::*sgRNA-neg* in pMTL-YN1C *catP*	This study
pDSW2055	P_{xyl}::*dCas9opt-*P_{gdh}::*sgRNA-cd630_17810-1* in pMTL-YN1C *catP*	This study
pDSW2057	P_{xyl}::*dCas9opt-*P_{gdh}::*sgRNA-cd630_17810-2* in pMTL-YN1C *catP*	This study
pIA33	P_{xyl}::*dCas9-opt* P_{gdh}::*sgRNA-rfp catP*	(26)
pIA34	P_{xyl}::*dCas9-opt* P_{gdh}::*sgRNA-neg catP*	(26)
pIA50	P_{xyl}::*dCas9-opt* P_{gdh}::*sgRNA-walA-1 catP*	This study
pIA51	P_{xyl}::*dCas9-opt* P_{gdh}::*sgRNA-walA-2 catP*	This study
pIA75	P_{xyl}::*walR* in pMTL-YN1C *catP*	This study
pIA76	P_{xyl}:*walR*^{D66E} in pMTL-YN1C *catP*	This study
pIA79	P_{xyl}::*dCas9-opt* P_{gdh}::*cd630_25040-1 catP*	This study
pIA80	P_{xyl}::*dCas9-opt* P_{gdh}::*cd630_25040-2 catP*	This study
pIA81	P_{xyl}::*dCas9-opt* P_{gdh}::*cd630_36010-1 catP*	This study
pIA93	P_{cdr_0665}::*mCherryOpt catP*	This study; *cdr_0665* is ortholog of *cd630_07380*

pIA95	P_{cdr_0796}::*mCherryOpt catP*	This study; *cdr_0796* is ortholog of *cd630_08670*
pIA97	P_{cdr_2753}::*mCherryOpt catP*	This study; *cdr_2753* is ortholog of *cd630_28620*
pIA98	P_{cdr_0455}::*mCherryOpt catP*	This study; *cdr_0455* is ortholog of *cd630_53000*
pIA100	P_{cd630_0739}::*mCherryOpt catP*	This study
pIA101	P_{cd630_0739}::*mCherryOpt* in pMTL-YN1C *catP*	This stduy
pIA102	P_{xyl}::*dCas9-opt* P_{gdh}::*cd630_05490 catP*	This study
pIA103	P_{xyl}::*dCas9-opt* P_{gdh}::*cd630_27940 catP*	This study
pIA104	P_{xyl}::*dCas9-opt* P_{gdh}::*cd630_27860 catP*	This study
pIA105	P_{xyl}::*dCas9-opt* P_{gdh}::*cd630_27910 catP*	This study
pIA106	P_{xyl}::*dCas9-opt* P_{gdh}::*cd630_10360 catP*	This study
pIA107	P_{pgdA}::*mCherryOpt catP*	This study
pIA108	P_{xyl}::*dCas9-opt* P_{gdh}::*cd630_07380-1 catP*	This study
pIA109	P_{xyl}::*dCas9-opt* P_{gdh}::*cd630_07380-2 catP*	This study
pIA110	P_{xyl}::*dCas9-opt* P_{gdh}::*cd630_07390-1 catP*	This study
pIA111	P_{xyl}::*dCas9-opt* P_{gdh}::*cd630_07390-2 catP*	This study
pIA112	P_{xyl}::*cd630_0738*	This study
pIA113	P_{xyl}::*cd630_0739*	This study
pIA114	P_{xyl}::*cd630_0738-cd630_0739*	This study
pIA115	P_{xyl}::*cd630_0739-cd630_0738*	This study
pMTL-YN1C	*E. coli-C. difficile* shuttle vector for inserting genes into *C. difficile* chromosome while restoring *pyrE*; *colE1 RP4oriT-TraJ CB102ori-repH' catP*	(29)

555 **Legends**

556 **Fig. 1. The *wal* operon of *C. difficile*.** Based on studies in other bacteria, WalK (red) is a bifunctional
557 signal transducing enzyme that can phosphorylate or dephosphorylate WalR (green). It is predicted to
558 have an extracellular Cache domain, as well as intracellular HAMP, HisKA (phospho-acceptor), and
559 HATPase domains. Unlike the *B. subtilis* ortholog (inset), it does not have an intracellular PAS domain.
560 WalR~P binds DNA to activate or repress expression of Wal-regulated genes. The lipoprotein (WalA,
561 blue), which is unique to *C. difficile*, may modulate WalK activity and is predicted to have a beta-propeller
562 lyase domain. The *truA2* gene codes for a pseudouridylate synthase and is not thought to play a role in
563 Wal signaling. Operon locus: *cdr20291_1676-1679* in R20291 and *cd630_17810-17840* in 630Δerm.

564

565 **Fig. 2. The *wal* operon is required for viability and normal rod morphology of *C. difficile* 630Δerm.**
566 (A) Viability assay. Serial dilutions of overnight cultures were spotted onto TY plates with or without 1%
567 xylose to induce the expression of *dCas9*. Plates were photographed after incubation overnight. Strains
568 carry chromosomal copies of the CRISPRi components and the following guides: sgRNA-neg (UM554),
569 sgRNA-*walA1* (UM555), and sgRNA-*walA2* (UM556). (B) Growth curves in liquid TY containing 0, 0.01,
570 0.1 or 1% xylose as indicated. For clarity, the sgRNA-neg control strain is graphed only at 0 xylose.
571 Samples were taken at 4 hours (arrow) for phase contrast microscopy (C), cell length measurements (D)
572 and determination of curvature (E). Numbers at the bottom of micrographs in (C) refer to % xylose. Note
573 cell debris indicative of lysis at 1% xylose. Bar = 10 μm. Cell length and percent curved cells were based
574 on about 500 cells per condition. The sgRNA-*walA1* strain is longer than the sgRNA-neg control in all
575 pairwise comparisons as determined by a T-test, $p<0.0001$.

576

577 **Fig. 3. Overexpression of *walR* from a multi-copy plasmid impairs growth, alters morphology and**
578 **slows autolysis in 630Δerm**. A. Viability assay. Overnight cultures of 630Δerm harboring pCE691
579 (P_{xyl}::*walR*) or the empty vector control plasmid pBZ101 (P_{xyl} EV) were serially diluted and spotted onto
580 TY-Thi plates with or without 1% xylose. Plates were photographed after incubation overnight. (B) Growth

581 curve of 630Δerm/pCE691 (P_{xyl}::*walR*). Duplicate cultures were grown to an OD_{600} of 0.2, at which time
582 one was induced with 3% xylose (green arrow). Both cultures were harvested after 3h (red arrow) for
583 analysis by phase contrast microscopy (C) and a lysis assay (D). Bar in (C) = 10 µm. For the lysis assay,
584 cells were suspended in buffer containing 0.01% Triton X-100 and OD_{600} was monitored over time. Error
585 bars depict SD of 3 technical replicates. Data shown are representative of at least 3 independent
586 experiments.
587
588 **Fig. 4. Prolonged overexpression of *walR* from a single-copy chromosomal P_{xyl}::*walR* allele**
589 **affects cell shape and slows lysis**. (A) Growth curves. An overnight culture of strain UM626 (P_{xyl}::*walR*
590 integrated at *pyrE* in 630Δerm) was subcultured 1:50 into TY with varied xylose concentrations as
591 indicated and grown for 6 hours, then analyzed in a lysis assay (B) or by phase contrast microscopy (C).
592 For the lysis assay, cells were suspended in buffer containing 0.01% Triton X-100 and OD_{600} was
593 monitored over time. Data are graphed as the mean and SD of 3 technical replicates, but most error bars
594 are smaller than the symbols. Cells from cultures grown in the presence of 0-1% xylose appeared normal
595 and are not shown, but in cultures induced with 3% xylose about 10% of the cells had irregular or bent
596 morphologies, examples of which are shown in (C). Bar = 10 µm. Data shown are representative of at
597 least 3 independent experiments.
598
599 **Fig. 5. Comparison of transcript changes between Wal-ON and Wal-OFF conditions**. (A). Heatmap
600 showing the 79 genes whose transcript abundance changed ≥ 4-fold when *walR* was overexpressed
601 (Wal-ON) in comparison to when the *wal* operon was silenced with CRISPRi (Wal-OFF). (B) Heatmap
602 showing the 49 genes whose transcript abundance changed ≥ 4-fold when the *wal* operon was silenced
603 (Wal-OFF) in comparison to when *walR* was overexpressed (Wal-ON). Green, induced. Red, repressed.
604

605 **Fig. 6. Confirmation of RNA-seq results with RFP reporter fusions to select genes.** Cells harboring
606 plasmids with transcriptional fusions of the red fluorescent protein mCherryOpt to the indicated promoters
607 were grown as per RNA-seq conditions, either Wal-ON (green) or Wal-OFF (red). Red fluorescence was
608 measured by flow cytometry and is graphed as the mean log2-fold change from two independent
609 experiments with two technical replicates. Error bars represent the SD of all four measurements. For
610 comparison, the mean log2-fold change of the same genes as determined by RNA-seq is also shown.
611 The *dltD* reporter is graphed only under Wal-OFF conditions because this fusion was induced by xylose
612 even in the absence of P_{xyl}::*walR*. Genes with asterisks denote fusions that were constructed to the
613 corresponding promoter regions from strain R20291.
614
615 **Fig. 7. Perturbation of individual Wal-ON regulon genes does not replicate the Wal-ON phenotype**.
616 Overnight cultures of 630Δerm harboring overexpression plasmids were subcultured into TY-Thi to an
617 OD_{600} of 0.03, grown to OD_{600} = 0.2 and induced with 3% xylose for 3h. Overnight cultures of 630Δerm
618 harboring CRISPRi plasmids were subcultured into TY-Thi containing 1% xylose to an OD_{600} of 0.03 and
619 grown to OD_{600} ~0.8. Each culture was then (A) examined by microscopy (bar 5 µm) and (B) tested in
620 the lysis assay. Induction of *walR* is the only condition that achieved phase bright cells and slowed lysis.
621 The plasmids used were: pBZ101 (EV), pCE691 (P_{xyl}::*walR*), pIA112 (P_{xyl}::*cd630_07380*), pIA113
622 (P_{xyl}::*cd630_07390*), pIA114 (P_{xyl}::*cd630_07380-07390*), pIA115 (P_{xyl}::*cd630_07390-07380*), pIA34
623 (sgRNA-neg), pCE744 (*sgRNA-cd630_27680-1*), and pCE745 (*sgRNA-cd630_27680-2*).
624
625 **Fig. 8. Perturbation of individual Wal-OFF regulon genes does not replicate the Wal-OFF**
626 **phenotype**. (A) Phase contrast microscopy of strains harboring overexpression plasmids or CRISPRi
627 plasmids after induction with xylose as described in the legend to Fig. 7. Bar = 5 µm. (B) Viability assay.
628 Overnight cultures were serially diluted and spotted onto TY plates with or without 1% xylose. Plates
629 were photographed after incubation overnight. CRISRPi knockdown of the *wal* operon was the only

630 condition that resulted in curved cells, lysis or a viability defect. The plasmids used were pBZ101 (EV),
631 pCE791 (P_{xyl}::*cwpV*), pIA34 (sgRNA-neg), pIA50 (sgRNA-*walA1*), and pCE738 (sgRNA-*dltD*).
632

633 **References**

634 1. Rohs PDA, Bernhardt TG. 2021. Growth and Division of the Peptidoglycan Matrix. Annu Rev
635 Microbiol 75:315-336.
636 2. Fabret C, Hoch JA. 1998. A two-component signal transduction system essential for growth of
637 *Bacillus subtilis*: implications for anti-infective therapy. J Bacteriol 180:6375-83.
638 3. Martin PK, Li T, Sun D, Biek DP, Schmid MB. 1999. Role in cell permeability of an essential
639 two-component system in *Staphylococcus aureus*. J Bacteriol 181:3666-73.
640 4. Dubrac S, Msadek T. 2004. Identification of genes controlled by the essential YycG/YycF two-
641 component system of *Staphylococcus aureus*. J Bacteriol 186:1175-81.
642 5. Dubrac S, Boneca IG, Poupel O, Msadek T. 2007. New insights into the WalK/WalR
643 (YycG/YycF) essential signal transduction pathway reveal a major role in controlling cell wall
644 metabolism and biofilm formation in *Staphylococcus aureus*. J Bacteriol 189:8257-69.
645 6. Ng WL, Robertson GT, Kazmierczak KM, Zhao J, Gilmour R, Winkler ME. 2003. Constitutive
646 expression of PcsB suppresses the requirement for the essential VicR (YycF) response
647 regulator in *Streptococcus pneumoniae* R6. Mol Microbiol 50:1647-63.
648 7. Ng WL, Kazmierczak KM, Winkler ME. 2004. Defective cell wall synthesis in *Streptococcus*
649 *pneumoniae* R6 depleted for the essential PcsB putative murein hydrolase or the VicR (YycF)
650 response regulator. Mol Microbiol 53:1161-75.
651 8. Dubrac S, Bisicchia P, Devine KM, Msadek T. 2008. A matter of life and death: cell wall
652 homeostasis and the WalKR (YycGF) essential signal transduction pathway. Mol Microbiol
653 70:1307-22.

654 9. Dubrac S, Msadek T. 2008. Tearing down the wall: peptidoglycan metabolism and the
655 WalK/WalR (YycG/YycF) essential two-component system. Adv Exp Med Biol 631:214-28.
656 10. Takada H, Yoshikawa H. 2018. Essentiality and function of WalK/WalR two-component system:
657 the past, present, and future of research. Biosci Biotechnol Biochem
658 doi:10.1080/09168451.2018.1444466:1-11.
659 11. Dobihal GS, Brunet YR, Flores-Kim J, Rudner DZ. 2019. Homeostatic control of cell wall
660 hydrolysis by the WalRK two-component signaling pathway in Bacillus subtilis. Elife 8.
661 12. Bisicchia P, Noone D, Lioliou E, Howell A, Quigley S, Jensen T, Jarmer H, Devine KM. 2007.
662 The essential YycFG two-component system controls cell wall metabolism in *Bacillus subtilis*.
663 Mol Microbiol 65:180-200.
664 13. Delauné A, Dubrac S, Blanchet C, Poupel O, Mader U, Hiron A, Leduc A, Fitting C, Nicolas P,
665 Cavaillon JM, Adib-Conquy M, Msadek T. 2012. The WalKR system controls major
666 staphylococcal virulence genes and is involved in triggering the host inflammatory response.
667 Infect Immun 80:3438-53.
668 14. Howell A, Dubrac S, Andersen KK, Noone D, Fert J, Msadek T, Devine K. 2003. Genes
669 controlled by the essential YycG/YycF two-component system of *Bacillus subtilis* revealed
670 through a novel hybrid regulator approach. Mol Microbiol 49:1639-55.
671 15. Liu X, Gallay C, Kjos M, Domenech A, Slager J, van Kessel SP, Knoops K, Sorg RA, Zhang JR,
672 Veening JW. 2017. High-throughput CRISPRi phenotyping identifies new essential genes in
673 *Streptococcus pneumoniae*. Mol Syst Biol 13:931.
674 16. Ng WL, Tsui HC, Winkler ME. 2005. Regulation of the pspA virulence factor and essential pcsB
675 murein biosynthetic genes by the phosphorylated VicR (YycF) response regulator in
676 *Streptococcus pneumoniae*. J Bacteriol 187:7444-59.
677 17. Delaune A, Poupel O, Mallet A, Coic YM, Msadek T, Dubrac S. 2011. Peptidoglycan
678 crosslinking relaxation plays an important role in *Staphylococcus aureus* WalKR-dependent cell
679 viability. PLoS One 6:e17054.

680 18. Takada H, Shiwa Y, Takino Y, Osaka N, Ueda S, Watanabe S, Chibazakura T, Su'etsugu M,
681 Utsumi R, Yoshikawa H. 2018. Essentiality of WalRK for growth in *Bacillus subtilis* and its role
682 during heat stress. Microbiology (Reading) 164:670-684.
683 19. CDC. 2019. Antibiotic Resistance Threats in the United States.
684 20. Fagan RP, Albesa-Jove D, Qazi O, Svergun DI, Brown KA, Fairweather NF. 2009. Structural
685 insights into the molecular organization of the S-layer from *Clostridium difficile*. Mol Microbiol
686 71:1308-22.
687 21. Fagan RP, Fairweather NF. 2014. Biogenesis and functions of bacterial S-layers. Nat Rev
688 Microbiol 12:211-22.
689 22. Kirk JA, Banerji O, Fagan RP. 2017. Characteristics of the *Clostridium difficile* cell envelope and
690 its importance in therapeutics. Microb Biotechnol 10:76-90.
691 23. Peltier J, Courtin P, El Meouche I, Lemee L, Chapot-Chartier MP, Pons JL. 2011. *Clostridium*
692 *difficile* has an original peptidoglycan structure with a high level of N-acetylglucosamine
693 deacetylation and mainly 3-3 cross-links. J Biol Chem 286:29053-62.
694 24. Nguyen HT, Wolff KA, Cartabuke RH, Ogwang S, Nguyen L. 2010. A lipoprotein modulates
695 activity of the MtrAB two-component system to provide intrinsic multidrug resistance, cytokinetic
696 control and cell wall homeostasis in *Mycobacterium*. Mol Microbiol 76:348-64.
697 25. Winkler ME, Hoch JA. 2008. Essentiality, bypass, and targeting of the YycFG (VicRK) two-
698 component regulatory system in gram-positive bacteria. J Bacteriol 190:2645-8.
699 26. Müh U, Pannullo AG, Weiss DS, Ellermeier CD. 2019. A xylose-inducible expression system
700 and a CRISPRi-plasmid for targeted knock-down of gene expression in *Clostridioides difficile*. J
701 Bacteriol doi:10.1128/jb.00711-18.
702 27. Dembek M, Barquist L, Boinett CJ, Cain AK, Mayho M, Lawley TD, Fairweather NF, Fagan RP.
703 2015. High-throughput analysis of gene essentiality and sporulation in *Clostridium difficile*. MBio
704 6:e02383.

705 28. Qi LS, Larson MH, Gilbert LA, Doudna JA, Weissman JS, Arkin AP, Lim WA. 2013.
706 Repurposing CRISPR as an RNA-guided platform for sequence-specific control of gene
707 expression. Cell 152:1173-83.
708 29. Ng YK, Ehsaan M, Philip S, Collery MM, Janoir C, Collignon A, Cartman ST, Minton NP. 2013.
709 Expanding the repertoire of gene tools for precise manipulation of the *Clostridium difficile*
710 genome: allelic exchange using *pyrE* alleles. PLoS One 8:e56051.
711 30. Fukuchi K, Kasahara Y, Asai K, Kobayashi K, Moriya S, Ogasawara N. 2000. The essential two-
712 component regulatory system encoded by *yycF* and *yycG* modulates expression of the *ftsAZ*
713 operon in *Bacillus subtilis*. Microbiology (Reading) 146 (Pt 7):1573-1583.
714 31. Lan CY, Igo MM. 1998. Differential expression of the OmpF and OmpC porin proteins in
715 *Escherichia coli* K-12 depends upon the level of active OmpR. J Bacteriol 180:171-4.
716 32. Caspi R, Billington R, Ferrer L, Foerster H, Fulcher CA, Keseler IM, Kothari A, Krummenacker
717 M, Latendresse M, Mueller LA, Ong Q, Paley S, Subhraveti P, Weaver DS, Karp PD. 2016. The
718 MetaCyc database of metabolic pathways and enzymes and the BioCyc collection of
719 pathway/genome databases. Nucleic Acids Res 44:D471-80.
720 33. Coullon H, Rifflet A, Wheeler R, Janoir C, Boneca IG, Candela T. 2020. Peptidoglycan analysis
721 reveals that synergistic deacetylase activity in vegetative *Clostridium difficile* impacts the host
722 response. J Biol Chem 295:16785-16796.
723 34. Kaus GM, Snyder LF, Müh U, Flores MJ, Popham DL, Ellermeier CD. 2020. Lysozyme
724 Resistance in *Clostridioides difficile* Is Dependent on Two Peptidoglycan Deacetylases. J
725 Bacteriol 202.
726 35. Ammam F, Patin D, Coullon H, Blanot D, Lambert T, Mengin-Lecreulx D, Candela T. 2020.
727 AsnB is responsible for peptidoglycan precursor amidation in *Clostridium difficile* in the
728 presence of vancomycin. Microbiology (Reading) 166:567-578.

729 36. Dajkovic A, Tesson B, Chauhan S, Courtin P, Keary R, Flores P, Marlière C, Filipe SR, Chapot-
730 Chartier MP, Carballido-Lopez R. 2017. Hydrolysis of peptidoglycan is modulated by amidation
731 of meso-diaminopimelic acid and Mg(2+) in *Bacillus subtilis*. Mol Microbiol 104:972-988.
732 37. Eveland SS, Pompliano DL, Anderson MS. 1997. Conditionally lethal *Escherichia coli* murein
733 mutants contain point defects that map to regions conserved among murein and folyl poly-
734 gamma-glutamate ligases: identification of a ligase superfamily. Biochemistry 36:6223-9.
735 38. Bradshaw WJ, Roberts AK, Shone CC, Acharya KR. 2018. The structure of the S-layer of
736 *Clostridium difficile*. J Cell Commun Signal 12:319-331.
737 39. Layec S, Decaris B, Leblond-Bourget N. 2008. Diversity of Firmicutes peptidoglycan hydrolases
738 and specificities of those involved in daughter cell separation. Res Microbiol 159:507-15.
739 40. Ho TD, Williams KB, Chen Y, Helm RF, Popham DL, Ellermeier CD. 2014. *Clostridium difficile*
740 extracytoplasmic function sigma factor sigmaV regulates lysozyme resistance and is necessary
741 for pathogenesis in the hamster model of infection. Infect Immun 82:2345-55.
742 41. Donahue EH, Dawson LF, Valiente E, Firth-Clark S, Major MR, Littler E, Perrior TR, Wren BW.
743 2014. *Clostridium difficile* has a single sortase, SrtB, that can be inhibited by small-molecule
744 inhibitors. BMC Microbiol 14:219.
745 42. Amoroso A, Boudet J, Berzigotti S, Duval V, Teller N, Mengin-Lecreulx D, Luxen A, Simorre JP,
746 Joris B. 2012. A peptidoglycan fragment triggers β-lactam resistance in *Bacillus licheniformis*.
747 PLoS Pathog 8:e1002571.
748 43. Sandhu BK, Edwards AN, Anderson SE, Woods EC, McBride SM. 2019. Regulation and
749 Anaerobic Function of the *Clostridioides difficile* β-Lactamase. Antimicrob Agents Chemother
750 64.
751 44. Dhiman A, Bhatnagar S, Kulshreshtha P, Bhatnagar R. 2014. Functional characterization of
752 WalRK: A two-component signal transduction system from *Bacillus anthracis*. FEBS Open Bio
753 4:65-76.

754 45. Woods EC, Nawrocki KL, Suárez JM, McBride SM. 2016. The *Clostridium difficile* Dlt Pathway
755 Is Controlled by the Extracytoplasmic Function Sigma Factor σ^V in Response to Lysozyme.
756 Infect Immun 84:1902-1916.
757 46. Fischer W, Rösel P, Koch HU. 1981. Effect of alanine ester substitution and other structural
758 features of lipoteichoic acids on their inhibitory activity against autolysins of *Staphylococcus*
759 *aureus*. J Bacteriol 146:467-75.
760 47. Wecke J, Perego M, Fischer W. 1996. D-alanine deprivation of *Bacillus subtilis* teichoic acids is
761 without effect on cell growth and morphology but affects the autolytic activity. Microb Drug
762 Resist 2:123-9.
763 48. McBride SM, Sonenshein AL. 2011. Identification of a genetic locus responsible for antimicrobial
764 peptide resistance in *Clostridium difficile*. Infect Immun 79:167-76.
765 49. Peschel A, Vuong C, Otto M, Götz F. 2000. The D-alanine residues of *Staphylococcus aureus*
766 teichoic acids alter the susceptibility to vancomycin and the activity of autolytic enzymes.
767 Antimicrob Agents Chemother 44:2845-7.
768 50. Sekulovic O, Ospina Bedoya M, Fivian-Hughes AS, Fairweather NF, Fortier LC. 2015. The
769 *Clostridium difficile* cell wall protein CwpV confers phase-variable phage resistance. Mol
770 Microbiol 98:329-42.
771 51. Ransom EM, Ellermeier CD, Weiss DS. 2015. Use of mCherry Red fluorescent protein for
772 studies of protein localization and gene expression in *Clostridium difficile*. Appl Environ
773 Microbiol 81:1652-60.
774 52. Fuchs M, Lamm-Schmidt V, Sulzer J, Ponath F, Jenniches L, Kirk JA, Fagan RP, Barquist L,
775 Vogel J, Faber F. 2021. An RNA-centric global view of *Clostridioides difficile* reveals broad
776 activity of Hfq in a clinically important gram-positive bacterium. Proc Natl Acad Sci U S A 118.
777 53. Dobihal GS, Flores-Kim J, Roney IJ, Wang X, Rudner DZ. 2021. The WalR-WalK signaling
778 pathway modulates the activities of both CwlO and LytE through control of the peptidoglycan
779 deacetylase PdaC in *Bacillus subtilis*. J Bacteriol doi:10.1128/jb.00533-21:Jb0053321.

780 54. Jansen A, Türck M, Szekat C, Nagel M, Clever I, Bierbaum G. 2007. Role of insertion elements
781 and yycFG in the development of decreased susceptibility to vancomycin in *Staphylococcus*
782 *aureus*. Int J Med Microbiol 297:205-15.
783 55. McEvoy CR, Tsuji B, Gao W, Seemann T, Porter JL, Doig K, Ngo D, Howden BP, Stinear TP.
784 2013. Decreased vancomycin susceptibility in Staphylococcus aureus caused by IS256
785 tempering of WalKR expression. Antimicrob Agents Chemother 57:3240-9.
786 56. Hu J, Zhang X, Liu X, Chen C, Sun B. 2015. Mechanism of reduced vancomycin susceptibility
787 conferred by *walK* mutation in community-acquired methicillin-resistant *Staphylococcus aureus*
788 strain MW2. Antimicrob Agents Chemother 59:1352-5.
789 57. Peng H, Hu Q, Shang W, Yuan J, Zhang X, Liu H, Zheng Y, Hu Z, Yang Y, Tan L, Li S, Hu X, Li
790 M, Rao X. 2017. WalK(S221P), a naturally occurring mutation, confers vancomycin resistance in
791 VISA strain XN108. J Antimicrob Chemother 72:1006-1013.
792 58. Hu Q, Peng H, Rao X. 2016. Molecular Events for Promotion of Vancomycin Resistance in
793 Vancomycin Intermediate *Staphylococcus aureus*. Front Microbiol 7:1601.
794 59. Mesnage S, Dellarole M, Baxter NJ, Rouget JB, Dimitrov JD, Wang N, Fujimoto Y, Hounslow
795 AM, Lacroix-Desmazes S, Fukase K, Foster SJ, Williamson MP. 2014. Molecular basis for
796 bacterial peptidoglycan recognition by LysM domains. Nat Commun 5:4269.
797 60. Neuhaus FC, Baddiley J. 2003. A continuum of anionic charge: structures and functions of D-
798 alanyl-teichoic acids in gram-positive bacteria. Microbiol Mol Biol Rev 67:686-723.
799 61. Rice KC, Bayles KW. 2008. Molecular control of bacterial death and lysis. Microbiol Mol Biol
800 Rev 72:85-109, table of contents.
801 62. Gibson DG, Young L, Chuang RY, Venter JC, Hutchison CA, 3rd, Smith HO. 2009. Enzymatic
802 assembly of DNA molecules up to several hundred kilobases. Nat Methods 6:343-5.
803 63. Dineen SS, Villapakkam AC, Nordman JT, Sonenshein AL. 2007. Repression of *Clostridium*
804 *difficile* toxin gene expression by CodY. Mol Microbiol 66:206-19.

805 64. Trieu-Cuot P, Carlier C, Poyart-Salmeron C, Courvalin P. 1991. Shuttle vectors containing a
806 multiple cloning site and a lacZ alpha gene for conjugal transfer of DNA from *Escherichia coli* to
807 gram-positive bacteria. Gene 102:99-104.
808 65. Kirk JA, Fagan RP. 2016. Heat shock increases conjugation efficiency in *Clostridium difficile*.
809 Anaerobe 42:1-5.
810 66. Ducret A, Quardokus EM, Brun YV. 2016. MicrobeJ, a tool for high throughput bacterial cell
811 detection and quantitative analysis. Nat Microbiol 1:16077.
812 67. Bolger AM, Lohse M, Usadel B. 2014. Trimmomatic: a flexible trimmer for Illumina sequence
813 data. Bioinformatics 30:2114-20.
814 68. Mende DR, Letunic I, Huerta-Cepas J, Li SS, Forslund K, Sunagawa S, Bork P. 2017.
815 proGenomes: a resource for consistent functional and taxonomic annotations of prokaryotic
816 genomes. Nucleic Acids Res 45:D529-d534.
817 69. Caspi R, Altman T, Billington R, Dreher K, Foerster H, Fulcher CA, Holland TA, Keseler IM,
818 Kothari A, Kubo A, Krummenacker M, Latendresse M, Mueller LA, Ong Q, Paley S, Subhraveti
819 P, Weaver DS, Weerasinghe D, Zhang P, Karp PD. 2014. The MetaCyc database of metabolic
820 pathways and enzymes and the BioCyc collection of Pathway/Genome Databases. Nucleic
821 Acids Res 42:D459-71.
822 70. Almagro Armenteros JJ, Tsirigos KD, Sonderby CK, Petersen TN, Winther O, Brunak S, von
823 Heijne G, Nielsen H. 2019. SignalP 5.0 improves signal peptide predictions using deep neural
824 networks. Nat Biotechnol 37:420-423.
825 71. Savojardo C, Martelli PL, Fariselli P, Profiti G, Casadio R. 2018. BUSCA: an integrative web
826 server to predict subcellular localization of proteins. Nucleic Acids Res 46:W459-w466.
827 72. Münch R, Hiller K, Grote A, Scheer M, Klein J, Schobert M, Jahn D. 2005. Virtual Footprint and
828 PRODORIC: an integrative framework for regulon prediction in prokaryotes. Bioinformatics
829 21:4187-9.

830 73. Hussain HA, Roberts AP, Mullany P. 2005. Generation of an erythromycin-sensitive derivative
831 of *Clostridium difficile* strain 630 (630Δe*rm*) and demonstration that the conjugative transposon
832 Tn*916*ΔE enters the genome of this strain at multiple sites. J Med Microbiol 54:137-41.

833

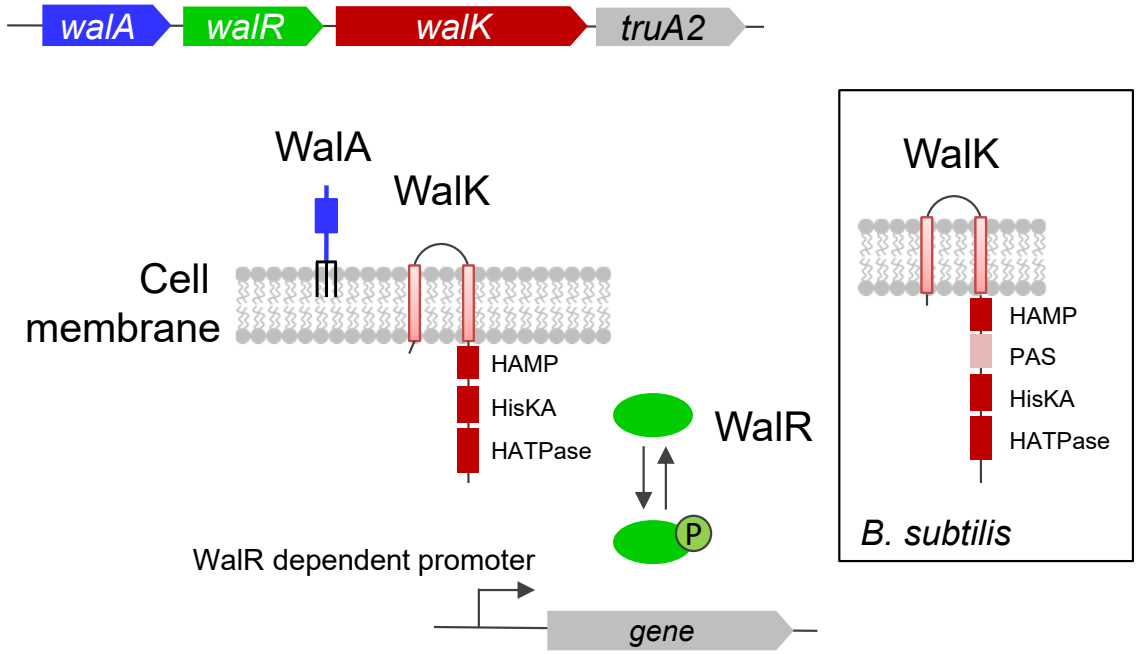

Fig. 1. The *wal* operon of *C. difficile*. Based on studies in other bacteria, WalK (red) is a bifunctional signal transducing enzyme that can phosphorylate or dephosphorylate WalR (green). It is predicted to have an extracellular Cache domain, as well as intracellular HAMP, HisKA (phospho-acceptor), and HATPase domains. Unlike the *B. subtilis* ortholog (inset), it does not have an intracellular PAS domain. WalR~P binds DNA to activate or repress expression of Wal-regulated genes. The lipoprotein (WalA, blue), which is unique to *C. difficile*, may modulate WalK activity and is predicted to have a beta-propeller lyase domain. The *truA2* gene codes for a pseudouridylate synthase and is not thought to play a role in Wal signaling. Operon locus: *cdr20291_1676-1679* in R20291 and *cd630_17810-17840* in 630Δerm.

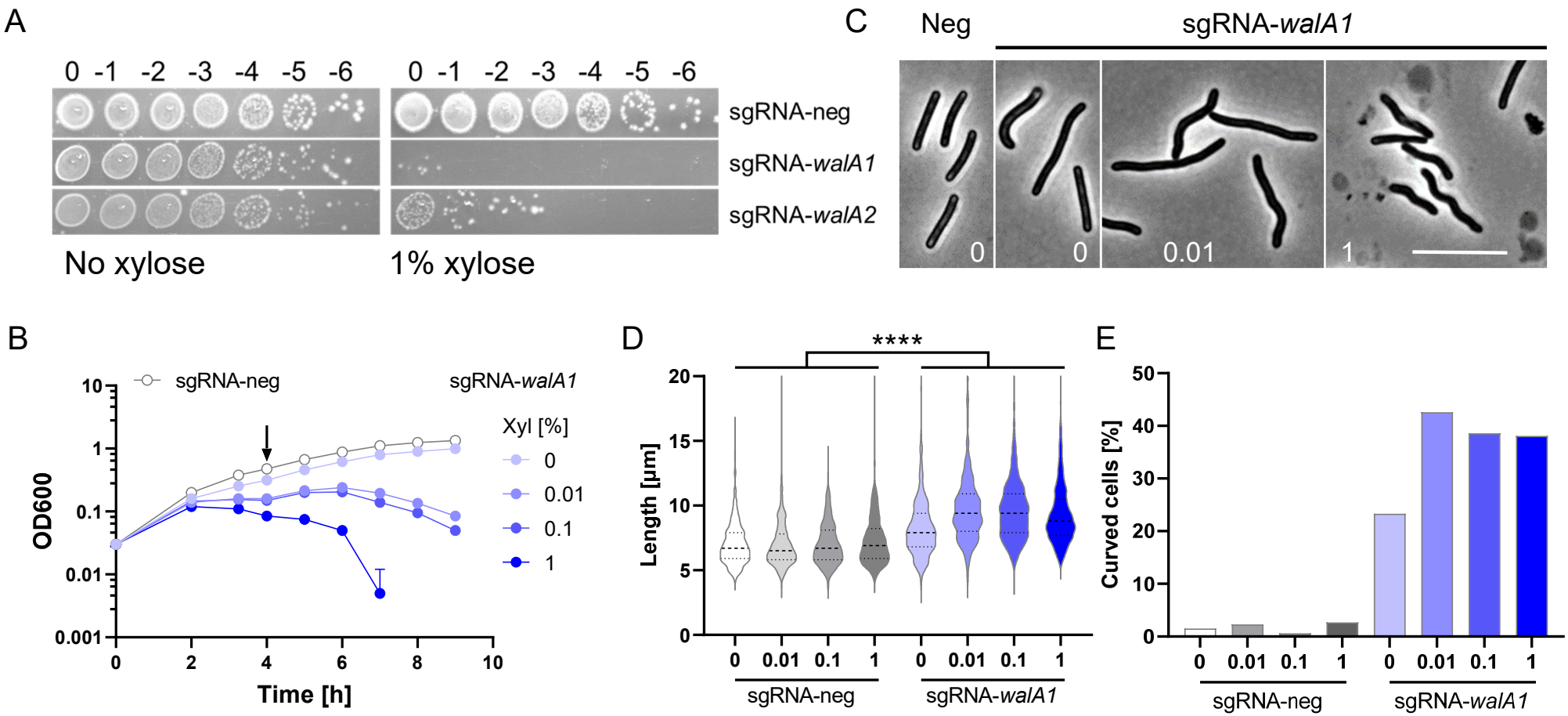

Fig. 2. The *wal* operon is required for viability and normal rod morphology of *C. difficile* 630Δerm. (A) Viability assay. Serial dilutions of overnight cultures were spotted onto TY plates with or without 1% xylose to induce the expression of *dCas9*. Plates were photographed after incubation overnight. Strains carry chromosomal copies of the CRISPRi components and the following guides: sgRNA-neg (UM554), sgRNA-*walA1* (UM555), and sgRNA-*walA2* (UM556). (B) Growth curves in liquid TY containing 0, 0.01, 0.1 or 1% xylose as indicated. For clarity, the sgRNA-neg control strain is graphed only at 0 xylose. Samples were taken at 4 hours (arrow) for phase contrast microscopy (C), cell length measurements (D) and determination of curvature (E). Numbers at the bottom of micrographs in (C) refer to % xylose. Note cell debris indicative of lysis at 1% xylose. Bar = 10 µm. Cell length and percent curved cells were based on about 500 cells per condition. The sgRNA-*walA1* strain is longer than the sgRNA-neg control in all pairwise comparisons as determined by a T-test, $p<0.0001$.

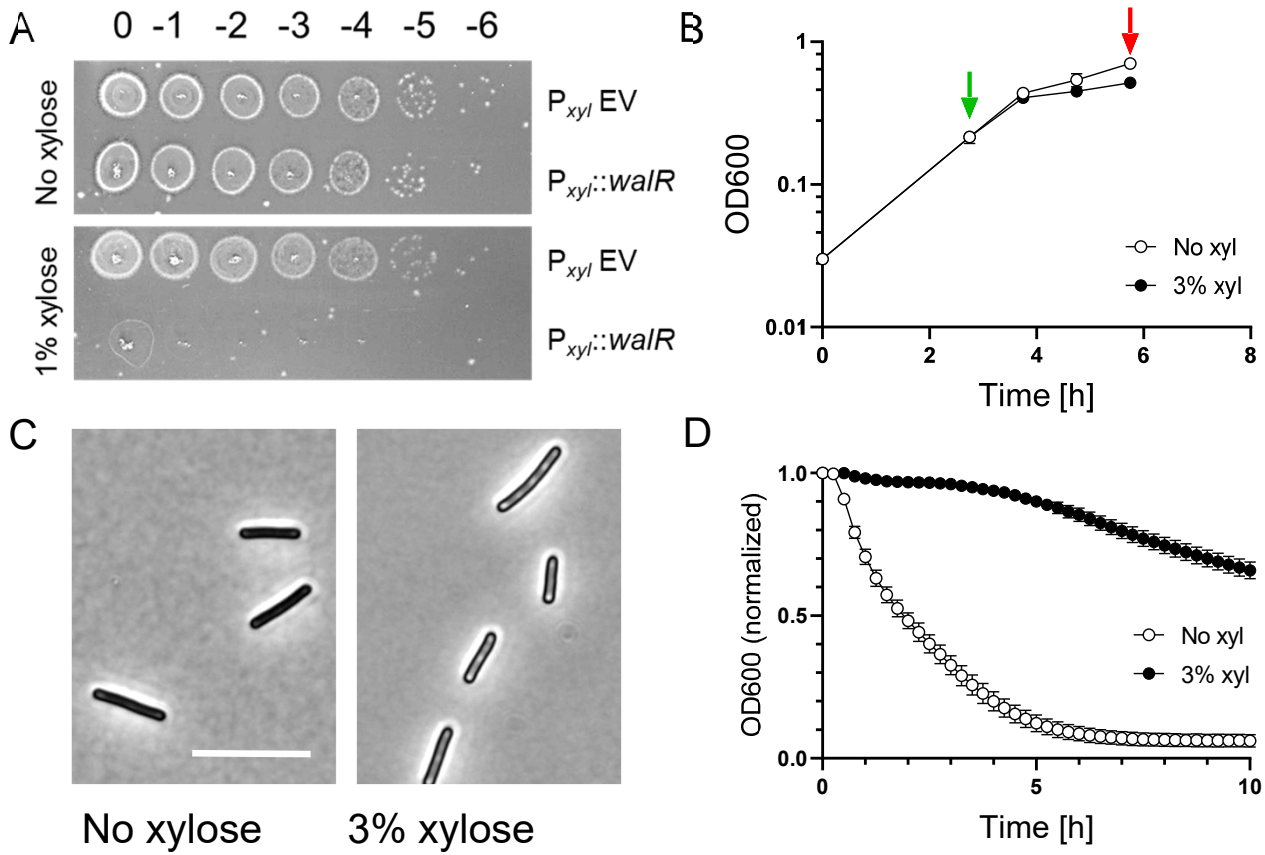

Fig. 3. Overexpression of *walR* from a multi-copy plasmid impairs growth, alters morphology and slows autolysis in 630Δerm. A. Viability assay. Overnight cultures of 630Δerm harboring pCE691 (P_{xyl}::*walR*) or the empty vector control plasmid pBZ101 (P_{xyl} EV) were serially diluted and spotted onto TY-Thi plates with or without 1% xylose. Plates were photographed after incubation overnight. (B) Growth curve of 630Δerm/pCE691 (P_{xyl}::*walR*). Duplicate cultures were grown to an OD_{600} of 0.2, at which time one was induced with 3% xylose (green arrow). Both cultures were harvested after 3h (red arrow) for analysis by phase contrast microscopy (C) and a lysis assay (D). Bar in (C) = 10 µm. For the lysis assay, cells were suspended in buffer containing 0.01% Triton X-100 and OD_{600} was monitored over time. Error bars depict SD of 3 technical replicates. Data shown are representative of at least 3 independent experiments.

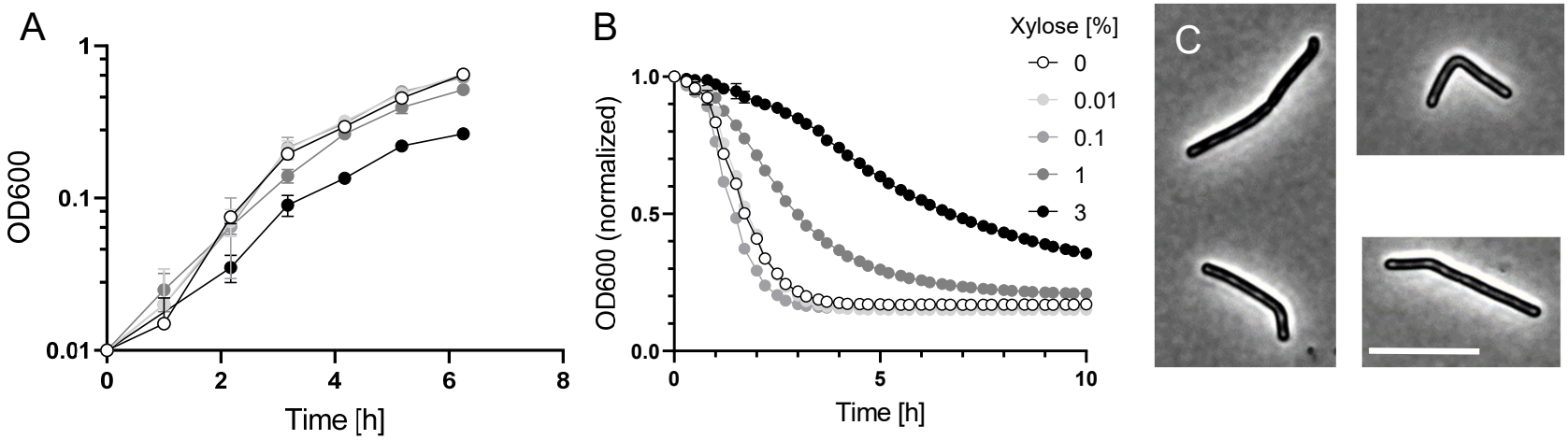

Fig. 4. Prolonged overexpression of *walR* from a single-copy chromosomal P_{xyl}::*walR* allele affects cell shape and slows lysis. (A) Growth curves. An overnight culture of strain UM626 (P_{xyl}::*walR* integrated at *pyrE* in 630Δerm) was subcultured 1:50 into TY with varied xylose concentrations as indicated and grown for 6 hours, then analyzed in a lysis assay (B) or by phase contrast microscopy (C). For the lysis assay, cells were suspended in buffer containing 0.01% Triton X-100 and OD_{600} was monitored over time. Data are graphed as the mean and SD of 3 technical replicates, but most error bars are smaller than the symbols. Cells from cultures grown in the presence of 0-1% xylose appeared normal and are not shown, but in cultures induced with 3% xylose about 10% of the cells had irregular or bent morphologies, examples of which are shown in (C). Bar = 10 µm. Data shown are representative of at least 3 independent experiments.

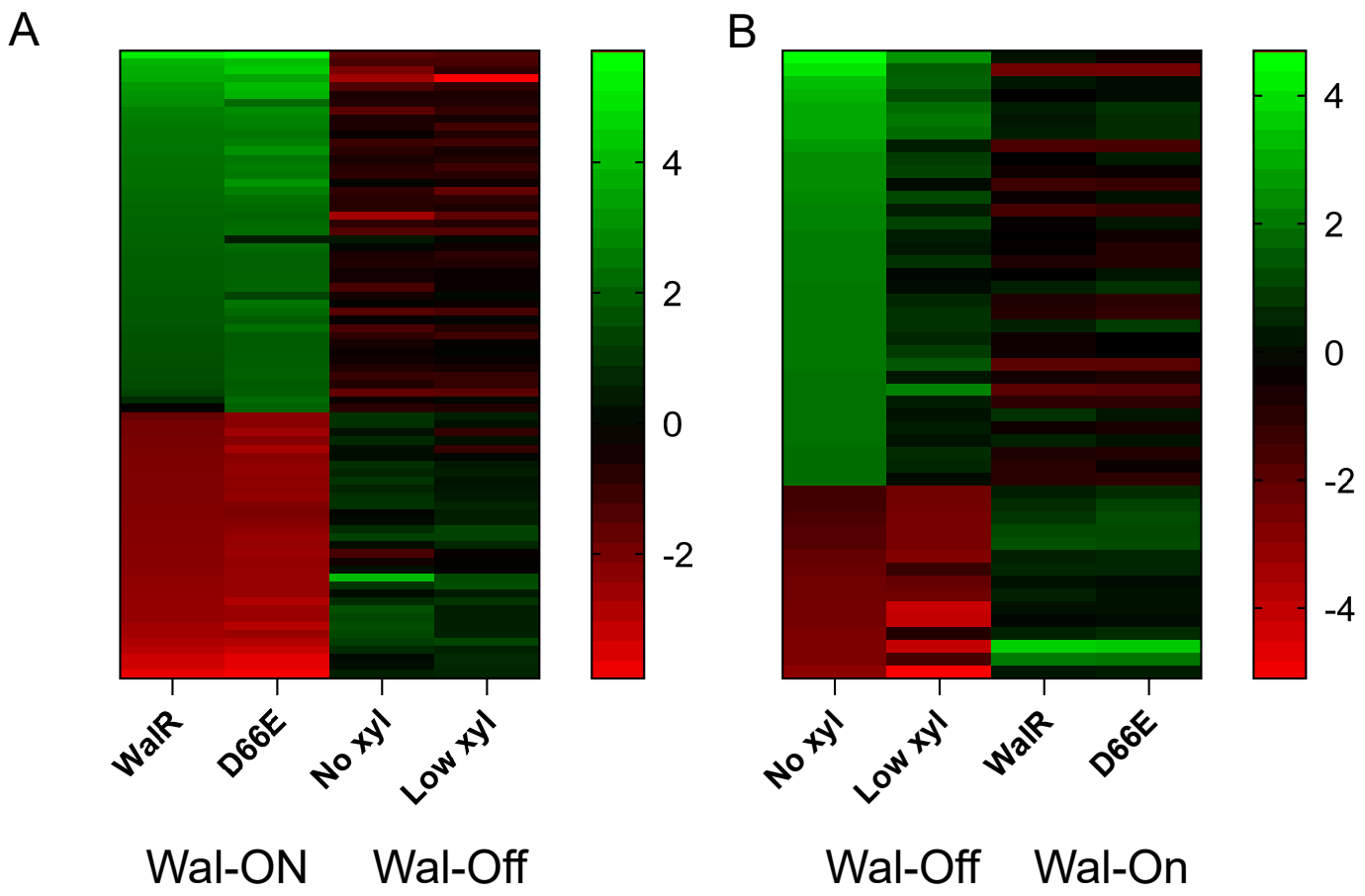

Fig. 5. Comparison of transcript changes between Wal-ON and Wal-OFF conditions. (A). Heatmap showing the 79 genes whose transcript abundance changed ≥ 4-fold when *walR* was overexpressed (Wal-ON) in comparison to when the *wal* operon was silenced with CRISPRi (Wal-OFF). (B) Heatmap showing the 49 genes whose transcript abundance changed ≥ 4-fold when the *wal* operon was silenced (Wal-OFF) in comparison to when *walR* was overexpressed (Wal-ON). Green, induced. Red, repressed.

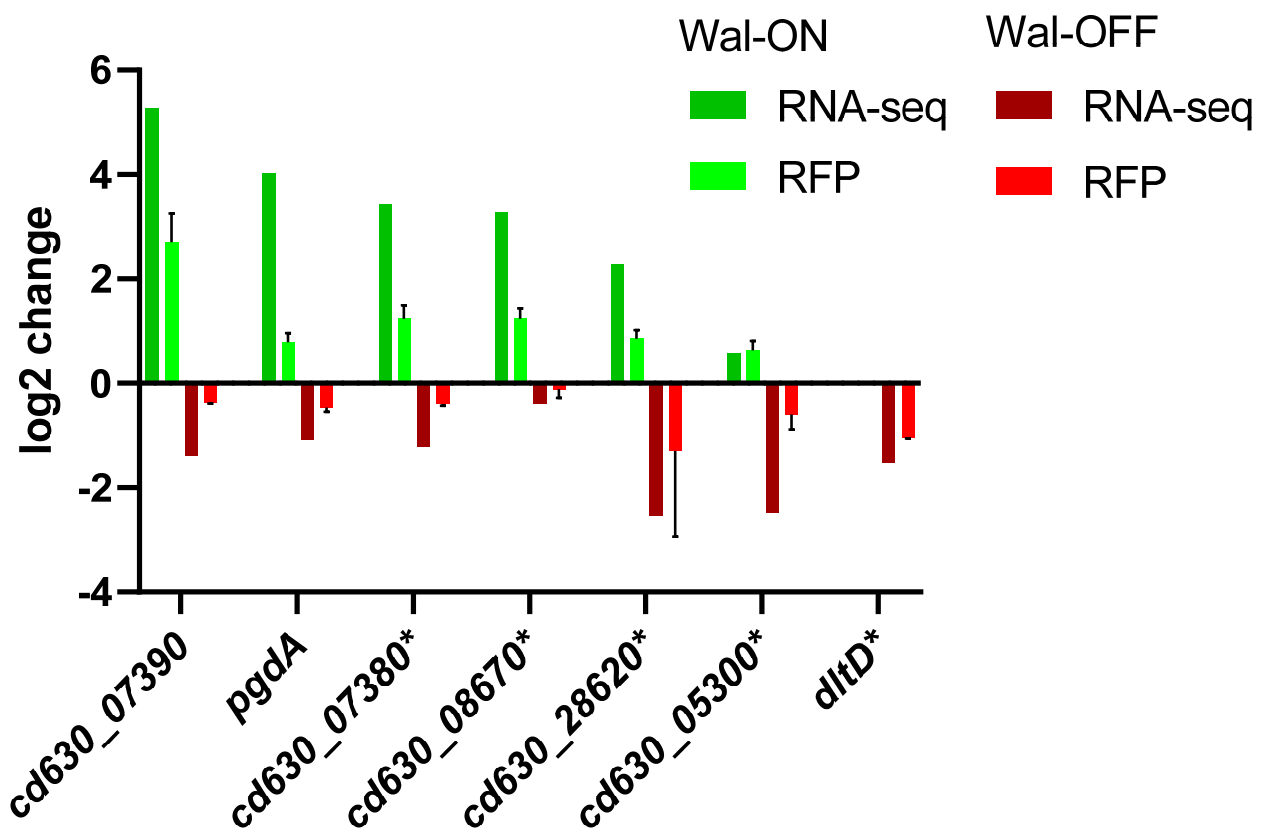

Fig. 6. Confirmation of RNA-seq results with RFP reporter fusions to select genes. Cells harboring plasmids with transcriptional fusions of the red fluorescent protein mCherryOpt to the indicated promoters were grown as per RNA-seq conditions, either Wal-ON (green) or Wal-OFF (red). Red fluorescence was measured by flow cytometry and is graphed as the mean log2-fold change from two independent experiments with two technical replicates. Error bars represent the SD of all four measurements. For comparison, the mean log2-fold change of the same genes as determined by RNA-seq is also shown. The *dltD* reporter is graphed only under Wal-OFF conditions because this fusion was induced by xylose even in the absence of P_{xyl}::*walR*. Genes with asterisks denote fusions that were constructed to the corresponding promoter regions from strain R20291.

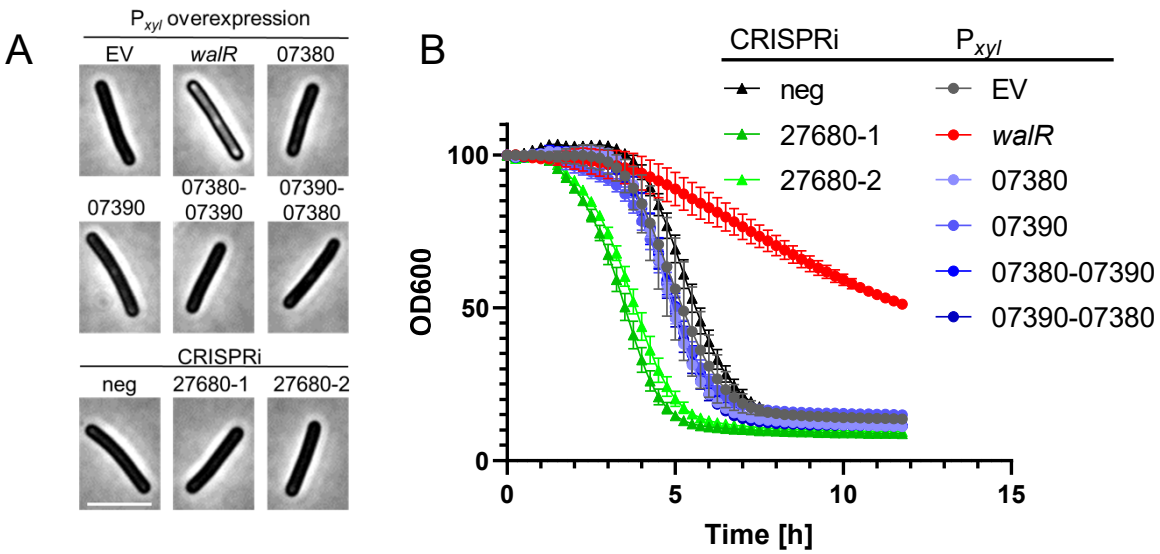

Fig. 7. Perturbation of individual Wal-ON regulon genes does not replicate the Wal-ON phenotype. Overnight cultures of 630Δerm harboring overexpression plasmids were subcultured into TY-Thi to an OD_{600} of 0.03, grown to OD_{600} = 0.2 and induced with 3% xylose for 3h. Overnight cultures of 630Δerm harboring CRISPRi plasmids were subcultured into TY-Thi containing 1% xylose to an OD_{600} of 0.03 and grown to OD_{600} ~0.8. Each culture was then (A) examined by microscopy (bar 5 µm) and (B) tested in the lysis assay. Induction of *walR* is the only condition that achieved phase bright cells and slowed lysis. The plasmids used were: pBZ101 (EV), pCE691 (P_{xyl}::*walR*), pIA112 (P_{xyl}::*cd630_07380*), pIA113 (P_{xyl}::*cd630_07390*), pIA114 (P_{xyl}::*cd630_07380-07390*), pIA115 (P_{xyl}::*cd630_07390-07380*), pIA34 (sgRNA-neg), pCE744 (*sgRNA-cd630_27680-1*), and pCE745 (*sgRNA-cd630_27680-2*).

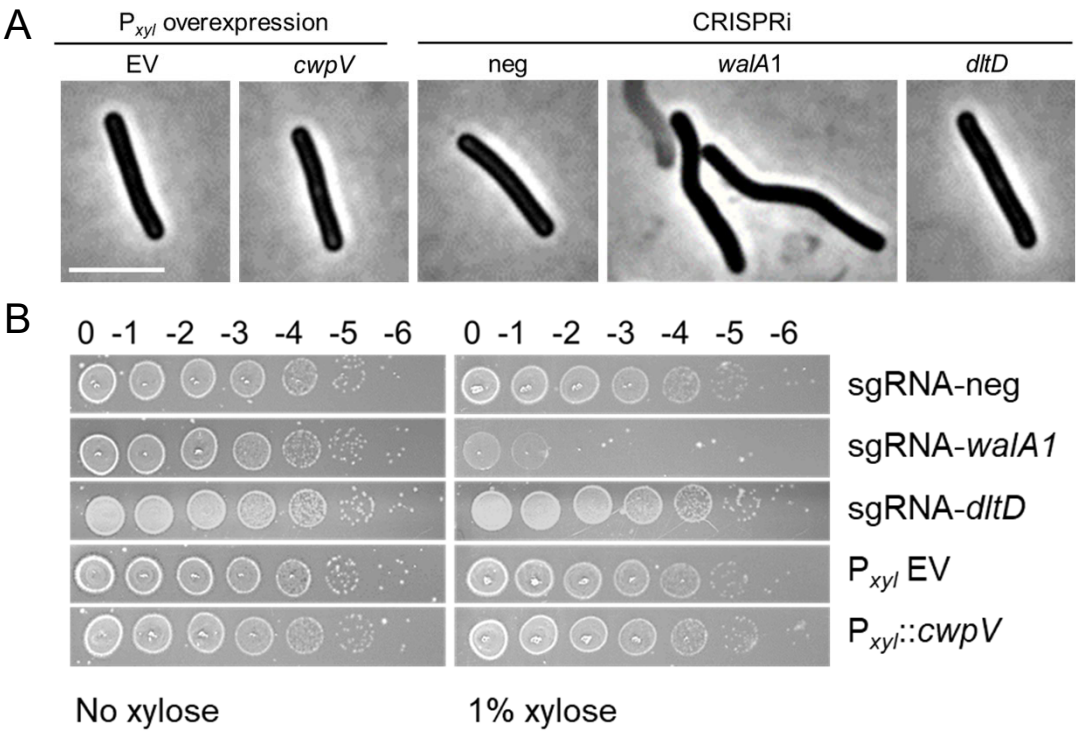

Fig. 8. Perturbation of individual Wal-OFF regulon genes does not replicate the Wal-OFF phenotype. (A) Phase contrast microscopy of strains harboring overexpression plasmids or CRISPRi plasmids after induction with xylose as described in the legend to Fig. 7. Bar = 5 µm. (B) Viability assay. Overnight cultures were serially diluted and spotted onto TY plates with or without 1% xylose. Plates were photographed after incubation overnight. CRISRPi knockdown of the *wal* operon was the only condition that resulted in curved cells, lysis or a viability defect. The plasmids used were pBZ101 (EV), pCE791 (P_{xyl}::*cwpV*), pIA34 (sgRNA-neg), pIA50 (sgRNA-*walA1*), and pCE738 (sgRNA-*dltD*).